

meso-Arylporpholactones and their Reduction Products

Christian Brückner,^{*,†} Junichi Ogikubo,[†] Jason R. McCarthy,^{†,‡} Joshua Akhigbe,[†] Michael A. Hyland,[†] Pedro Daddario,[†] Jill L. Worlinsky,[†] Matthias Zeller,[§] James T. Engle,^{||} Christopher J. Ziegler,^{||} Matthew J. Ranaghan,[⊥] Megan N. Sandberg,[†] and Robert R. Birge^{†,⊥}

[†]Department of Chemistry, University of Connecticut, Storrs, Connecticut 06269-3060, United States

[⊥]Department of Molecular and Cell Biology, University of Connecticut, Storrs, Connecticut 06269-3125, United States

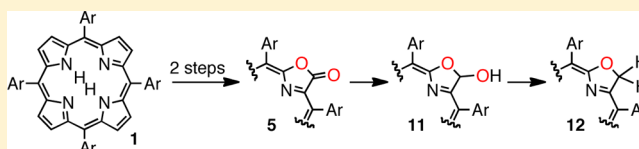
[§]Department of Chemistry, Youngstown State University, One University Plaza, Youngstown, Ohio 44555-3663, United States

^{||}Department of Chemistry, University of Akron, Akron, Ohio 44325-3601, United States

S Supporting Information

ABSTRACT: The rational syntheses of *meso*-tetraaryl-3-oxo-2-oxaporphyrins **5**, known as porpholactones, via MnO_4^- -mediated oxidations of the corresponding *meso*-tetraaryl-2,3-dihydrochlorins (**7**) is detailed. Since chlorin **7** is prepared from the parent porphyrin **1**, this amounts to a 2-step replacement of a pyrrole moiety in **1** by an oxazolone moiety.

The stepwise reduction of the porpholactone **5** results in the formation of chlorin analogues, *meso*-tetraaryl-3-hydroxy-2-oxachlorin (**11**) and *meso*-tetraaryl-2-oxachlorins (**12**). The reactivity of **11** with respect to nucleophilic substitution by O-, N-, and S-nucleophiles is described. The profound photophysical consequences of the formal replacement of a pyrrole with an oxazolone (porphyrin-like chromophore) or (substituted) oxazole moiety (chlorin-like chromophore with, for the parent oxazolochlorin **12**, red-shifted Q_x band with enhanced oscillator strengths) are detailed and rationalized on the basis of SAC-CI and MNDO-PSDCI molecular orbital theory calculations. The single crystal X-ray structures of the porpholactones point at a minor steric interaction between the carbonyl oxygen and the flanking phenyl group. The essentially planar structures of all chromophores in all oxidation states prove that the observed optical properties originate from the intrinsic electronic properties of the chromophores and are not subject to conformational modulation.



INTRODUCTION

meso-Tetraarylporphyrins **1** and their metal complexes are used in a number of model compounds for naturally occurring porphyrinic cofactors or light-harvesting systems.¹ The great popularity of **1** arises from their straightforward syntheses and the availability of a wide variety of aryl-functionalized derivatives.²

In a seminal contribution by Crossley and King more than 25 years ago,³ it was recognized that oxidation of β -substituted porphyrins, such as dione **6** (prepared from **1** via **2**, **3**, or **4**), can lead to the loss of one β -carbon and the formal replacement of the porphyrinic β,β' -bond by a lactone moiety, forming porpholactone **5** (Scheme 1).

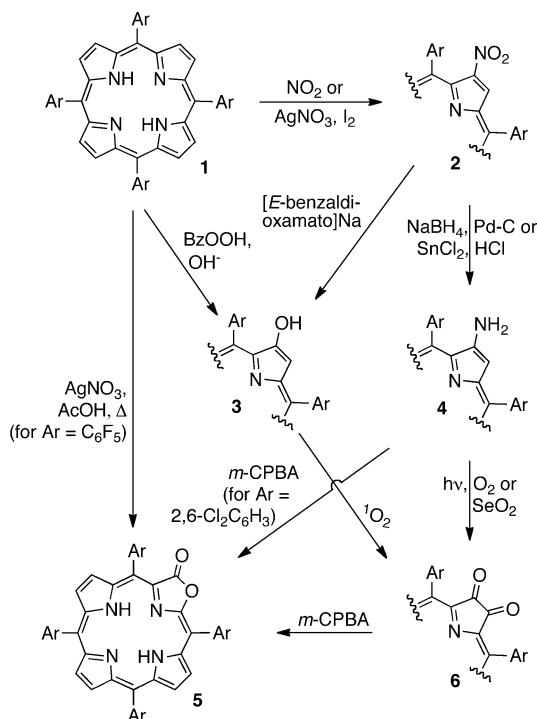
One other serendipitous finding five years later identified strongly oxidizing reaction conditions (AgNO_3 in refluxing acetic acid containing oxalate) that were suitable for converting porphyrin **1** (with $\text{Ar} = \text{C}_6\text{F}_5$) directly into a porpholactone.^{4,5} However, the latter reaction is not general since it is only applicable toward the synthesis of *meso*-tetrakis-(pentafluorophenyl)porpholactone. The method also requires extensive chromatography to separate the porpholactone from the starting material and numerous other nonpolar “over-oxidized” byproducts.^{4,5} Additional specialized reaction pathways toward porpholactones have been discovered since, such as the singlet oxygen oxidation of β -aminoporphyrin **4** (Scheme

1).⁶ Select oxidations of dione **6** also lead to porpholactones, perhaps shedding light on a possible reaction mechanism toward the formation of porpholactones **5**.⁷ Porpholactones also appeared as adventitious products in a variety of oxidation reactions of β -derivatized porphyrins.^{7–9}

Porpholactones have been demonstrated to be of practical value: The Fe(III) and Fe(IV)=O complexes of *meso*-tetrakis(2,6-dichlorophenyl)-substituted porpholactone were used as model compounds for naturally occurring chlorin-type prosthetic groups.⁶ The catalytic activity of the Fe(III)Cl and Mn(III)Cl complexes of *meso*-tetraphenylporpholactone with respect to olefin epoxidation and sulfide oxidation reactions were tested.^{10,11} [*meso*-Tetrakis(pentafluorophenyl)porpholactonato]Pt(II) is a promising component in pressure sensitive paints,¹² allowing the imaging of air flow around objects.¹³ This complex can also be utilized as a high pH sensor in the range of pH 11.5–13.¹⁴ Despite their increasing utility and the emergence of their unique reactivity, no full account on the rational, general, and high-yielding synthesis of *meso*-tetraarylporpholactones has been published to date. In the first part of this report, we will fill this gap by following on our communication.¹⁵

Received: May 18, 2012

Published: June 26, 2012

Scheme 1. Literature-known Syntheses of Porpholactone 5^a

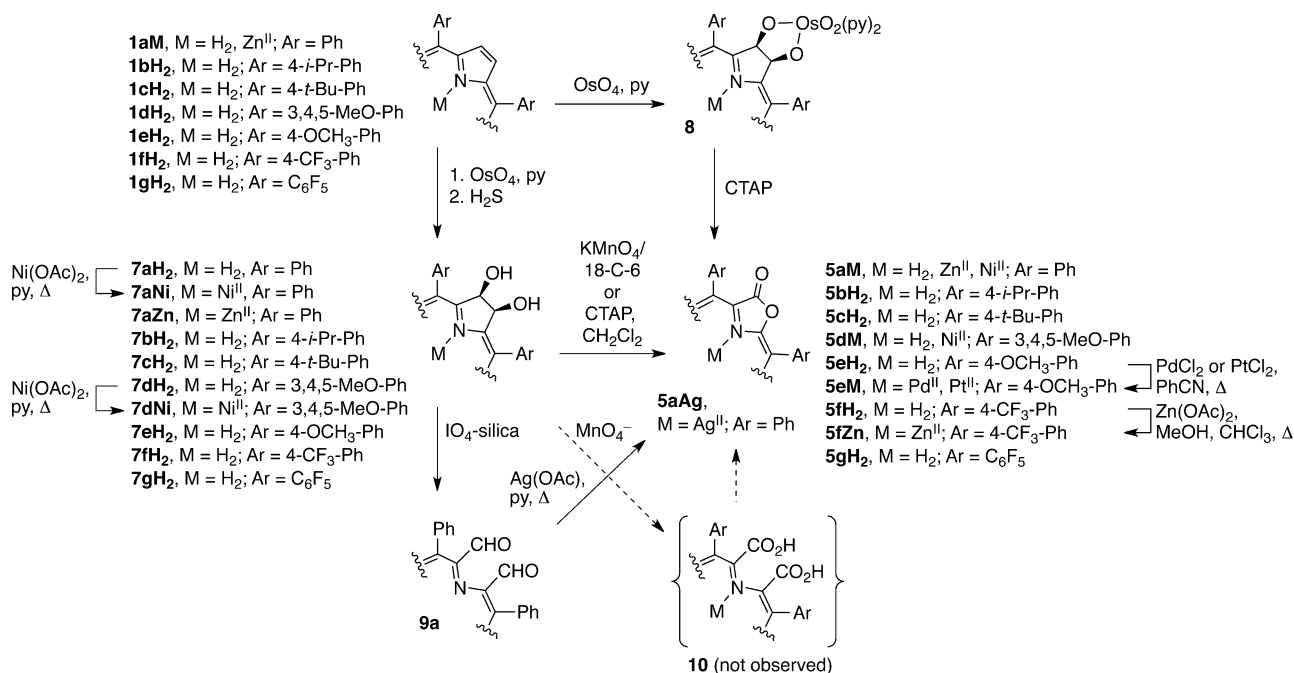
^aOnly free bases are shown but some transformations may require metal complexation, or metal insertion takes place during the transformation.

We previously detailed the OsO₄-mediated β,β'-dihydroxylation of *meso*-tetraarylporphyrin **1** and closely related porphyrin derivatives to produce the corresponding *meso*-tetraaryl-2,3-dihydroxy-2,3-chlorin **7**.^{14,16–20} This reaction was adopted by other groups, providing a range of dihydroxy-chlorins.^{10,11,21–23} We further demonstrated the versatility of

the chlorin diols as starting material for the preparation of porphyrinoids containing nonpyrrolic building blocks using our versatile “breaking and mending” strategy.^{9,14–18,24,25} The synthesis of porpholactones via the MnO₄⁻-mediated oxidation of the known *meso*-tetraaryl-2,3-dihydroxychlorin follows this strategy as well. We will also present the structural description of free base and Zn(II) porpholactones using single crystal X-ray diffraction structure elucidation.

In the second part of this report we present a comprehensive account of the hydride-mediated reduction reactions of porpholactones **5** to chlorin-like 2-oxachlorins (also known as oxazolochlorins) containing hemiacetal, acetal, and ether functionalities. Owing to their intense absorbance at wavelengths >650 nm, the optical window of tissue,²⁶ chlorins (β,β'-dihydroporphyrins) are superior to porphyrins in all applications in which light needs to penetrate tissue, such as the photodynamic therapy (PDT) of tumors.²⁷ In addition, many naturally occurring light-harvesting chromophores are chlorins.²⁸ In part owing to these applications, the generation of chlorins by total synthesis or by conversion of porphyrins has become a central topic in current porphyrin chemistry.²⁹

We previously presented an isolated example of a reduced porpholactone derivative, hemiacetal 3-hydroxy-2-oxachlorin **11H₂**, in a comparative study of chlorins,³⁰ and we demonstrated that this compound possesses high photodynamic efficacy *in vivo* in a murine tumor model.³¹ We also identified an adventitious side-product in the oxidative transformations of the silver(II) complex of dihydroxychlorin **7** as an [2-ethoxy-2-oxachlorinato]Ag(II) complex (**11aAg**).^{8,32} Lastly, an oxazolochlorin monomer and dimer formed as products of an intramolecular Cannizzaro reaction of free base secochlorin bisaldehyde **9aM**.⁹ However, in spite of their use or occurrence on several occasions, no full synthetic paper describing their rational syntheses has been reported to date. This will be provided herein, and we will also provide chemical evidence that might rationalize the high biological activity of the hemiacetal.³¹

Scheme 2. Synthesis of Porpholactones **5** by Oxidation of 2,3-Dihydroxychlorins **7**

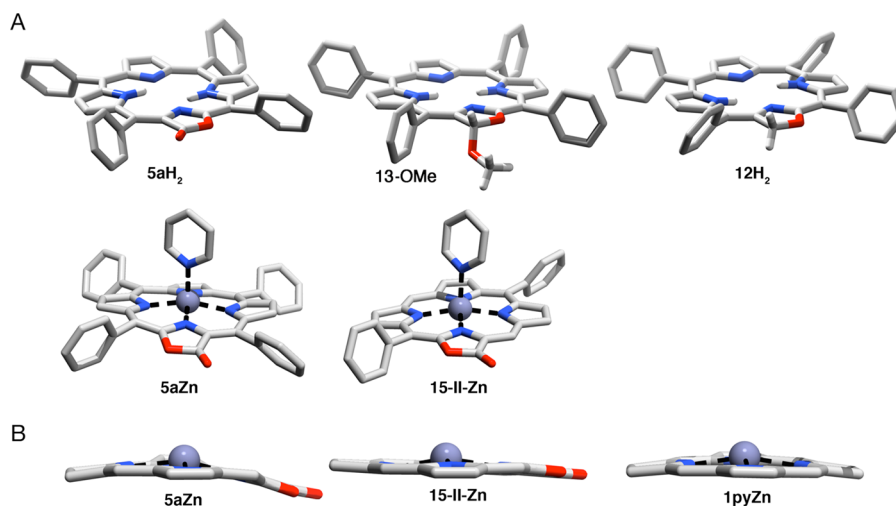


Figure 1. Single crystal X-ray structures of porpholactone **5aH₂**, [porpholactonato]Zn(py) **5aZn**, 2-oxachlorin **12H₂**, 3-methoxy-2-oxachlorin **13-OMe**, and [diphenylporpholactonato]Zn(py) **15-II-Zn**. A. Oblique views; all solvates, disorder, and hydrogen atoms attached to sp²-carbons removed for clarity. B. Side view of the porpholactones **5aH₂** and **15-II-Zn** in comparison to the chromophore of [meso-tetrakis(4-pyridyl)porphyrinato]Zn(pyridine) **1pyZn**; meso-aryl substituents, axially coordinated pyridine (if present), and hydrogen atoms attached to sp²-carbons removed for clarity. See ESI for details on the crystal structure analyses.

In the final section of this manuscript, we will contrast the UV–visible absorption and fluorescence emission properties of the free base and Zn(II) complexes of the 2-oxaporphyrin and 2-oxachlorin against each other and against the properties of the parent porphyrin **1a** and 2,3-dihydroxychlorin **7aH₂**. The observed trends in the optical spectra are rationalized on the basis of SAC–CI and MNDO-PSDCI molecular orbital theory calculations. Thus, this contribution reveals the synthesis and detailed physical and chemical description of a chlorin-like stable family of chromophores that is readily accessible and for which a number of applications can be foreseen.

RESULTS AND DISCUSSION

Synthesis of Porpholactones. Oxidation of dihydroxychlorins **7** with MnO₄[−] produced porpholactone **5** in a single step (Scheme 2). The source of MnO₄[−] can either be an excess of powdered KMnO₄ suspended at ambient temperature in an organic solvent (toluene, CH₂Cl₂, CHCl₃, THF) in the presence of the phase-transfer agent 18-crown-6, KMnO₄ heterogenized on silica gel,³³ or, most conveniently, the use of 1–5 equivalents of cetyltrimethylammonium permanganate (CTAP)³⁴ in CH₂Cl₂.

The workup of the reaction is simple. Filtration of the crude mixture through a plug of diatomaceous earth removes the brown, flocculent to pasty manganese oxides. Short column chromatography and crystallization of the porpholactone isolates the product as crystalline materials in up to 90% yields. The reaction times vary, depending on the concentration (and solubility) of the dihydroxychlorin and the number of equivalents of CTAP (or phase transfer agent) used, and range from 30 min to 12 h. The addition of several smaller portions of oxidant while monitoring the consumption of the starting material by TLC proved to be beneficial. Large excesses of oxidant, elevated temperatures or prolonged reaction times hasten the degradation of the macrocycles, as indicated by the loss of the Soret band in the UV–visible spectra of the reaction mixtures, and low isolated yields of the desired porpholactones.

We recently described the isolation of the dihydroxychlorin osmate esters **8**, the primary products from the reaction of

porphyrin **1** with OsO₄.¹⁹ The osmate esters are also susceptible to CTAP oxidation to the corresponding porpholactones but the reaction is slower than the reaction of the corresponding alcohols, and the fate of the osmium is not clear. Given the high toxicity of OsO₄ that potentially forms as a side product,³⁵ the oxidation of the diol is given preference over the oxidation of the corresponding osmate ester. We reported the CTAP oxidation of the osmate ester of meso-tetrakis(pentafluorophenyl)-2,3-dihydroxychlorin **7gH₂**.¹⁴ The reason for this was that the corresponding diol could at the time not be prepared. Since then, we have reported a method for the preparation of the **7gH₂**,³⁶ and we found that the oxidation of this diol is faster and cleaner than the oxidation of its osmate ester. Also, we will report here that the use of permanganate heterogenized on silica gel offers a very convenient and clean way of generating this meso-tetrakis(pentafluorophenyl)porpholactone **5gH₂** (and it allows facile recovery of starting material). In general, however, the yields of this reaction are very low (25–30% are typical) compared to the yields obtained from oxidation of other tetraaryldihydroxychlorins.

The isolation of the porpholactones by silica gel column chromatography is much facilitated by their lower polarity compared to the corresponding dihydroxychlorins. Their identification is simplified by their characteristic mass and NMR spectra, indicative of the loss of one carbon from the porphyrin framework, the loss of axial symmetry, and the presence of a carbonyl group. As noted previously,^{3,4} the UV–visible spectra of free base porpholactones are surprisingly porphyrin-like, while those of their metal complexes are metallochlorin-like (to be detailed below).

We consider this methodology toward porpholactones to be fairly general. It is applicable to the oxidation of free base dihydroxychlorin **7**, its Ni(II), Zn(II), Ag(II), and Pt(II) complexes, to diol chlorins carrying a variety of electron-donating and -withdrawing meso-phenyl substituents,¹⁴ and 5,15-diphenyl-2,3-dihydroxychlorin **14** (see below). We previously also demonstrated the applicability of this method to the synthesis of dithiaporphyrin- and porphyrin *N*-oxide-based porpholactones.^{17,18} As also shown previously,^{6,10–12} additional

metalloporpholactones are available through metal insertions into the free bases using standard methods (using conventional and microwave heating).

The exact mechanism of formation of the porpholactones remains unclear. Permanganate oxidation of dihydroxychlorin **7** suggests the formation of secochlorin bis-carboxylate **10**. In fact, Crossley already surmised that the as yet unobserved secochlorin **10** is the immediate precursor to porpholactone **5**.³ Other reactions that reasonably can be expected to produce the bis-carboxylate species also generate porpholactones. For instance, an attempt to insert silver ions into free base bisaldehyde **9** (using excess Ag(I) in pyridine, heat) formed [porpholactonato]Ag(II) **5Ag** in mediocre yield (~20%). Independent evidence points toward 2,3-dioxochlorins of type **6** to be the key intermediates in the conversion of porpholactones.^{7,18} Since porpholactones frequently also appear as adventitious (by)products in a number of reactions that treat (β -derivatized) porphyrins under a variety of oxidizing conditions,^{3,4,7,8} one may regard porpholactones as the thermodynamic sink in the β, β' -oxidative degradation pathway of porphyrins. As such, it can be reasonably assumed that multiple pathways lead to this product.

Structural Aspects of Porpholactones. The crystal structures of [porpholactonato]Mn(III)Cl,¹⁰ Fe(III)Cl,⁶ Cu(II),⁷ and Ni(II)⁷ complexes are known. Thus, the connectivity of the porpholactones is not in question. However, the crystal structures of free base porpholactone **5aH₂** and its Zn complex **5aZn** are interesting with respect to a number of other aspects (Figure 1A). The structural relationship of **5aH₂** to the corresponding porphyrin **1aH₂**³⁷ is highlighted by the fact that both structures possess essentially isostructural unit cell parameters: same space group $P\bar{1}$, with the cell dimension varying by only ~1% when comparing the room temperature structure of **1aH₂** to the structure of **5aH₂** determined at 100 K. The chromophore of porpholactone **5aH₂** is, analogous to that of porphyrin **1aH₂**, in effect planar with only a minor waving deformation ($wav(x)$) of the two opposing pyrrole moieties that is likely caused by the repulsion of the two inner hydrogens.³⁸ Like the metalloporpholactone crystal structures described today (see below), the free base porpholactone structure is highly disordered with respect to the relative position of the lactone moiety. In **5aH₂**, all 8 possible positions/orientations are occupied, albeit in a nonstatistical manner (for details, see Supporting Information). While this highlights the structural equivalency of the replacement of a β, β' -bond by a lactone moiety, it also diminishes the significance of small bond lengths and angles differences. We therefore will consider herein mostly general structural trends.

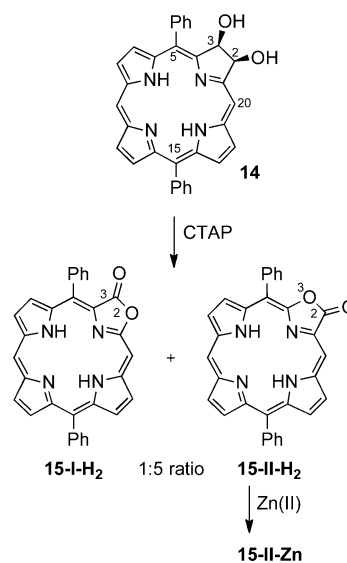
A comparison of the Ni(II), Cu(II), Fe(III), and Mn(III) complexes of porphyrins³⁹ and porpholactones^{6,7,10} show also their overall similarity with respect to the overall macrocycle conformation. The C=O bond length in the zinc porpholactone **5aZn** is 1.26 Å and the C–O bond length is 1.40 Å. The corresponding bond lengths in the Mn(III)Cl complex of **5a** are 1.20 and 1.40 Å.¹⁰

Figure 1B shows a side view of the macrocycles of [porpholactonato]Zn(II) **5aZn** and its porphyrin analogue **1pyZn** ([*meso*-tetrakis(4-pyridyl)porphyrinato]Zn(pyridine))⁴⁰ (and the diphenylporpholactone **15-II-Zn**, described below). The zinc ion sits in all complexes slightly out of plane, drawn toward the side of the axially coordinated pyridine. This is normally observed for square pyramidal zinc(II) porphyrin complexes.³⁹ Most notably when comparing the conformations

of the macrocycles in **5aZn** and **1pyZn**, the oxazolone moiety is not, as expected, perfectly coplanar with the macrocycle. This deviation may originate from a steric interaction between the carbonyl oxygen and the flanking phenyl group. A comparable observation was made for the Cu(II) complex of tetraphenylporpholactone.⁷

To test whether other experimental evidence can be found for a significant steric interaction between the lactone carbonyl and the flanking phenyl group, we subjected the known diphenyl-2,3-dihydroxychlorin **14**²³ to the CTAP oxidation conditions (Scheme 3). Two isomers of the corresponding diphenylporpholactone **15** can be formed: 2-oxa-3-oxo structure **15-I-H₂**, and 3-oxa-2-oxo structure **15-II-H₂**.

Scheme 3. Synthesis of Diphenylporpholactone Regioisomers 15-I-H₂ and 15-II-H₂



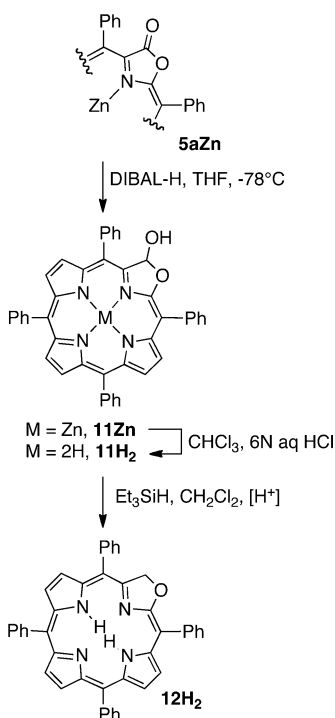
The oxidation of diol **14** proceeded smoothly and rapidly, generating a porpholactone product mixture. The ¹H NMR of the porpholactone fraction indicated the presence of two isomers in a ~1:5 ratio (see SI). Repeated preparative plate chromatography and recrystallizations (from MeOH/CHCl₃) allowed the isolation of a pure fraction of the majority product but the minority product could not be isolated in pure and high enough yields to perform a full analysis. 1D and 2D-NMR spectroscopy (see SI) allowed the unambiguous assignment of the majority product as the 2-oxo-3-oxa isomer **15-II-H₂**, that is unaffected by any steric interaction between the lactone carbonyl and a phenyl group. This was confirmed by single X-ray crystal structure elucidation of **15-II-Zn**, as its pyridine adduct, formed by zinc insertion into the free base (Figure 1).

The fact that the seemingly less sterically inhibited isomer forms in preference over the other isomer serves as an indication for the existence of a small but noticeable steric interaction between the carbonyl and the phenyl group. Most significantly, the macrocycle conformation (Figure 1B) shows that the lactone moiety is near-perfectly coplanar with the oxazole moiety and that the macrocycle of **15-II-Zn** is overall significantly more planar than that of the tetraaryl analogue **5aZn**. This provides the most convincing proof for the rationalization of the nonplanar arrangements of the lactone moiety with the porphyrins in **5aH₂** and **5aZn** on steric grounds.

In addition, we observed reduced disorder in the structure of **15-II-Zn** versus that observed in **5aZn**, and thus can more reliably determine the bond lengths in the oxazolone ring. The C=O lengths in **15-II-Zn** range from 1.106(3) to 1.228(3) Å, while the C–O lengths vary between 1.357(3) to 1.486(8) Å (there are two independent molecules per unit cell).

Step-wise Reduction of Porpholactone 5aZn. Functional group conversions of the lactone moiety offer the opportunity to synthesize oxazolochlorins.^{9,25,30,31} Thus, reduction of the nonpolar purple porpholactone **5aZn** with DIBAL-H in dry THF at -78°C generates in near-quantitative yields a bright blue-green pigment of much higher polarity (isolated yields $\sim 80\%$, 1 g scale; Scheme 4). The ^1H NMR

Scheme 4. Step-wise Reduction of Porpholactones 5



spectroscopic signature of this product is lactone-like with two additional signals: One signal of variable chemical shift assigned to the hydroxy functionality (exchangeable with D_2O), and a signal at 3.62 ppm attributed to the proton of the oxazole-moiety (cf. to the pyrroline proton of **7aZn** at 6.12 ppm).¹⁶ The corresponding sp^3 -carbon signal is observed at 112.1 ppm in the ^{13}C NMR spectrum. All other analytical and spectroscopic data confirm the structure of the reduction product to be [3-hydroxy-2-oxachlorinato]Zn **11Zn**.

The reduction of free base porpholactones (**5H₂**) is complicated by the formation of aluminum-containing side products. Low valent aluminum species are known to metalate free base porphyrins.⁴¹ Therefore, the free base porpholactol **11H₂** is best prepared by reduction of the zinc complex **5aZn**, whereby the workup procedure includes a wash with 6 M aqueous HCl that demetalates the product.

The hemiacetal functionality of **11H₂** is susceptible to acetal formation under mild conditions.^{8,9} Hence, alcohols must be excluded from any isolation and/or manipulation procedure of **11H₂/Zn**, lest the formation of the corresponding acetals are desired (see also below).

An acid-catalyzed ($\text{BF}_3\cdot\text{OEt}_2$ or Amberlyst 15, H^+ form) silane-induced deoxygenation of the lactol hydroxy group of **11H₂** (or **11Zn** concomitant with a demetalation reaction) at room temperature provides a green compound that can be identified as the oxazolochlorin **12H₂**. The loss of the hydroxyl group from **11H₂** is marked by a decrease in polarity of the product, the appearance of the signals in the ^1H NMR at 6.54 ppm for the two oxazolochlorin protons, accompanied by the signal in the ^{13}C NMR for a secondary carbon (DEPT) at 76.4 ppm (see SI).

The connectivity of 2-oxachlorin **12H₂** could be determined by single crystal X-ray diffraction (Figure 1A). As expected, the chromophore is planar with none of the nonplanarity observed in the porpholactones **5**. However, the extraordinary degree of disorder of the molecule in the crystal precludes any detailed bond length and angle analysis.

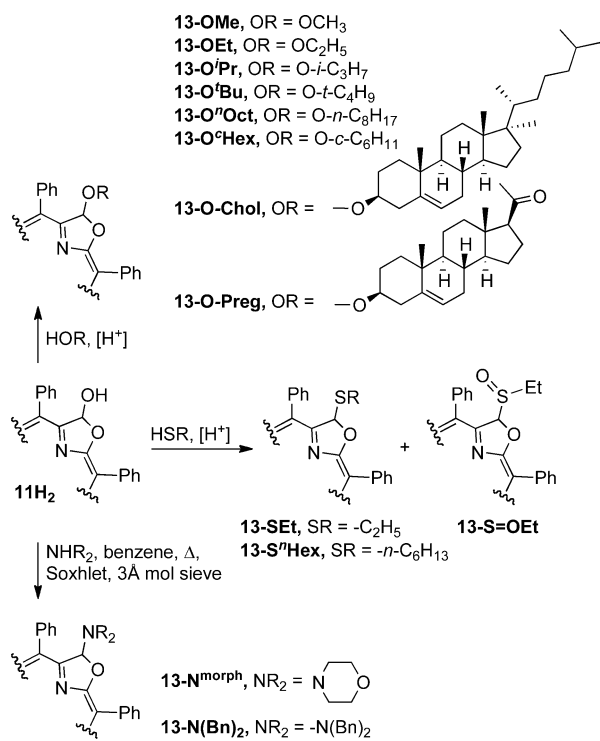
2-Oxachlorin **12H₂** is generally sensitive toward (photo-sensitized) oxidation back to porpholactol **11H₂**. Thus, the compound must be shielded from exposure to light or oxidizing conditions. The oxazole methylene group is located in a benzylic position with respect to the porphyrinoid aromatic system and α to an oxygen atom in the oxazole moiety. This group thus is highly activated with respect to, for instance, carbocation formation, a fact highlighted by an oxidative dimerization reaction of an oxazolochlorin that is proposed to be an intermediate in the Cannizzaro reaction of *meso*-phenylsecochlorin bisaldehyde.⁹ As a result of this high reactivity, insertion of zinc(II) into **12H₂** requires anaerobic conditions. Warming **12H₂** with $\text{Zn}(\text{OAc})_2\cdot 2\text{H}_2\text{O}$ in degassed warm DMF under N_2 leads cleanly to the formation of **12Zn**. The optical properties of the oxazolochlorin derivatives are discussed below.

Attempts at one-step reductions from **5aZn** to **12aZn** using LiAlH_4 or DIBAL-H under more forcing conditions (large stoichiometric excess, room temperature) failed. These reactions merely lead to the destruction of the porphyrinic macrocycle without the formation of any major product.

Acetalization of Porpholactol 11H₂. The lactol hydroxy group of **11H₂** is susceptible to facile acid-catalyzed nucleophilic substitution by a range of O-, N-, and S-nucleophiles, providing access to a number of stable chlorin-like derivatives of graded lipophilicity (Scheme 4). A marked nucleophile-dependent reactivity difference is noted. Exposure of **11H₂** to primary, secondary, and tertiary alcohols results in a rapid reaction that is essentially quantitative after 30 min to 1 h at ambient temperature. The resulting acetals **13-OR** showed all the expected spectroscopic data (Scheme 5). Diagnostic for the successful formation of acetals containing an α -methylene group, this group shows a diastereotopic splitting in its ^1H NMR spectra. This can be rationalized by its relative position with respect to the macrocycle plane,³² exposing one of the methylene protons to a much larger degree to the diatropic ring current than the other. Alkoxy-substituted morpholinochlorins show a very similar effect.^{15,16} Bulky alcohols like cholesterol or pregnenolone can also be attached to the chromophore with ease.

The crystal structure of **13-OMe**, as its $\text{Ag}(\text{II})$ complex,³² and a porpholactol acetal dimer⁹ were previously characterized by single crystal X-ray diffraction. We present here the structure of **13-OMe** as a proof of connectivity and to complete the series of 2-oxachlorins in three different oxidation states (together with the 3-oxo- and the 3-hydroxy-2-oxachlorins), but the structure is disordered to a point that a conformational

Scheme 5. Derivatization of Porpholactol 11H₂ by Nucleophilic Substitution of the Lactol Hydroxy Group



analysis is meaningless. The conformation of the oxazolochlorin chromophore in the dimer, however, suggested a certain degree of conformational flexibility, though no major distortions from planarity were observed.⁹

Secondary amines required a longer reaction time and azeotropic removal of the water formed (reflux in benzene with 3 Å mol sieves placed in a Soxhlet apparatus over several days) to push the reaction to completion. The hemiaminals **13-NR₂** showed all the expected spectroscopic and analytical properties, including the diastereotopic split of the α -methylene protons. We did not succeed in reacting primary amines with the porpholactols under these or other conditions tested.

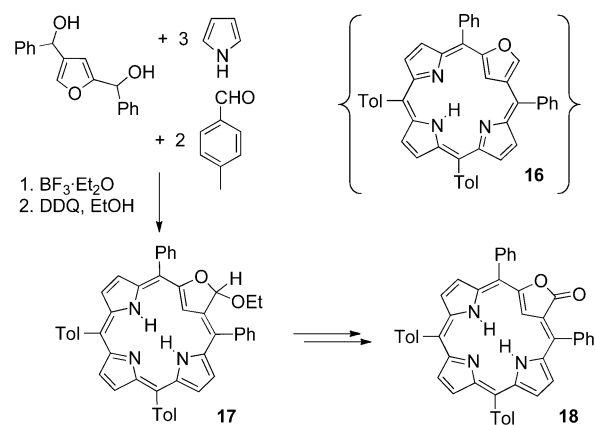
The reactivity of primary thiols was very much similar to the reactivity of the corresponding alcohols. Over time, however, the formation of side products with spectroscopic data suggestive of being the corresponding sulfoxides appeared (m/z = +16 compared to the expected compound; essentially identical ¹H and ¹³C NMR spectra).

This high reactivity of lactol **11H₂** with respect to acetal, aminal, and thioacetal formation is of immediate interest for the potential application of the 2-oxachlorins as photochemotherapeutics. We previously demonstrated the efficacy of **11H₂** when incorporated into a biodegradable nanoparticle for the photodynamic treatment of a tumor in a mouse model.³¹ The facile acetalization demonstrated here suggests that the biodistribution of the hemiacetal may also be modulated by its ability to undergo derivatization with biomolecules containing alcohol and thiol groups. Such promiscuity may allow achievement of a biodistribution of the drug it would not have as a single and stable compound. Inversely, the facile derivatization of the 3-hydroxy-2-oxachlorins suggests the preparation of amphiphilic (pro)drugs using PEGs, carbohydrates, or similarly suitable moieties. These aspects of the oxazolochlorins are currently being studied in detail.

Comparison of Porpholactones and Oxazolochlorins to their Carbaporphyrin Analogues.

Carbaporphyrins are porphyrin analogues containing a carbon atom in place of an inner nitrogen. Pawlicki and Latos-Grazynski reported the total synthesis of **17**, the carbaporphyrin analogue to 3-methoxy-2-oxachlorin **13-OEt**.^{44,45} This reaction is in contrast to our “breaking and mending of porphyrin” strategy toward porpholactones **5**. Like **13-OEt** (see below), 2-oxa-21-carbachlorin **17** possesses a chlorin-like spectrum (λ_{Soret} = 437 nm and four Q-bands with λ_{max} = 672 nm). The synthesis of the free base nonmacrocycle-aromatic 2-oxa-21-carbaporphyrin could not be achieved. Multistep oxidation of **17** led to the formation of porphyrinoid **18**, the carbaporphyrin analogue to porpholactone **5** (Scheme 6). The UV–visible spectrum of

Scheme 6. Synthesis of 2-Oxa-21-carbaporphyrin 16, 2-Oxa-21-carbachlorin 17, and 2-Oxa-3-oxo-21-carbaporphyrin 18



18 is, in similar fashion to its aza-analogue, porphyrin-like with a sharp Soret band and four Q-bands (λ_{max} = 690 nm). Unlike the azaporphyrins, however, the metallocarbaporphyrin chemistry is dominated by reactions on the inner carbon.⁴⁶

Optical Properties of Porpholactones and Oxazolochlorins. Free base porpholactones possess UV–visible and fluorescence emission spectra that are almost indistinguishable from those of the corresponding porphyrins (Figure 2). The similarity of the porphyrin and porpholactone spectra, noted already upon their discovery,^{3,4} is surprising as the modified pyrrolic moiety has lost its cross-conjugated β, β' -double bond. Therefore, porpholactones could have been expected to possess chlorin-like spectra.⁴² Evidently, however, the electronic effects of the carbonyl double bond mimic the presence of a β, β' -double bond. On the other hand, porpholactone Zn(II) complexes exhibit metallochlorin-like UV–visible spectra, though they are slightly hypsochromically shifted when compared to the spectra for metallochlorin **7aZn**. On the basis of iterative extended Hückel calculations, Gouterman and co-workers categorized porpholactones to lie between porphyrins and chlorins.⁴

The reduced porpholactones, 3-hydroxy-2-oxachlorins **11H₂** (λ_{max} = 646 nm) and **11Zn**, both possess chlorin-like optical spectra (cf. to the spectra for **7aH₂**, λ_{max} = 648 nm, and **7aZn**). The influence of the 3-hydroxyl functionality on the 2-oxachlorin chromophore is profound. The removal of this group in the free base chromophore **12H₂** results in a 22 nm red-shift (λ_{max} = 668 nm) in the UV–visible spectrum. We have demonstrated before the distinct blue-shifts caused by OH-substitution of chlorin pyrroles.¹⁹ Most surprisingly, the

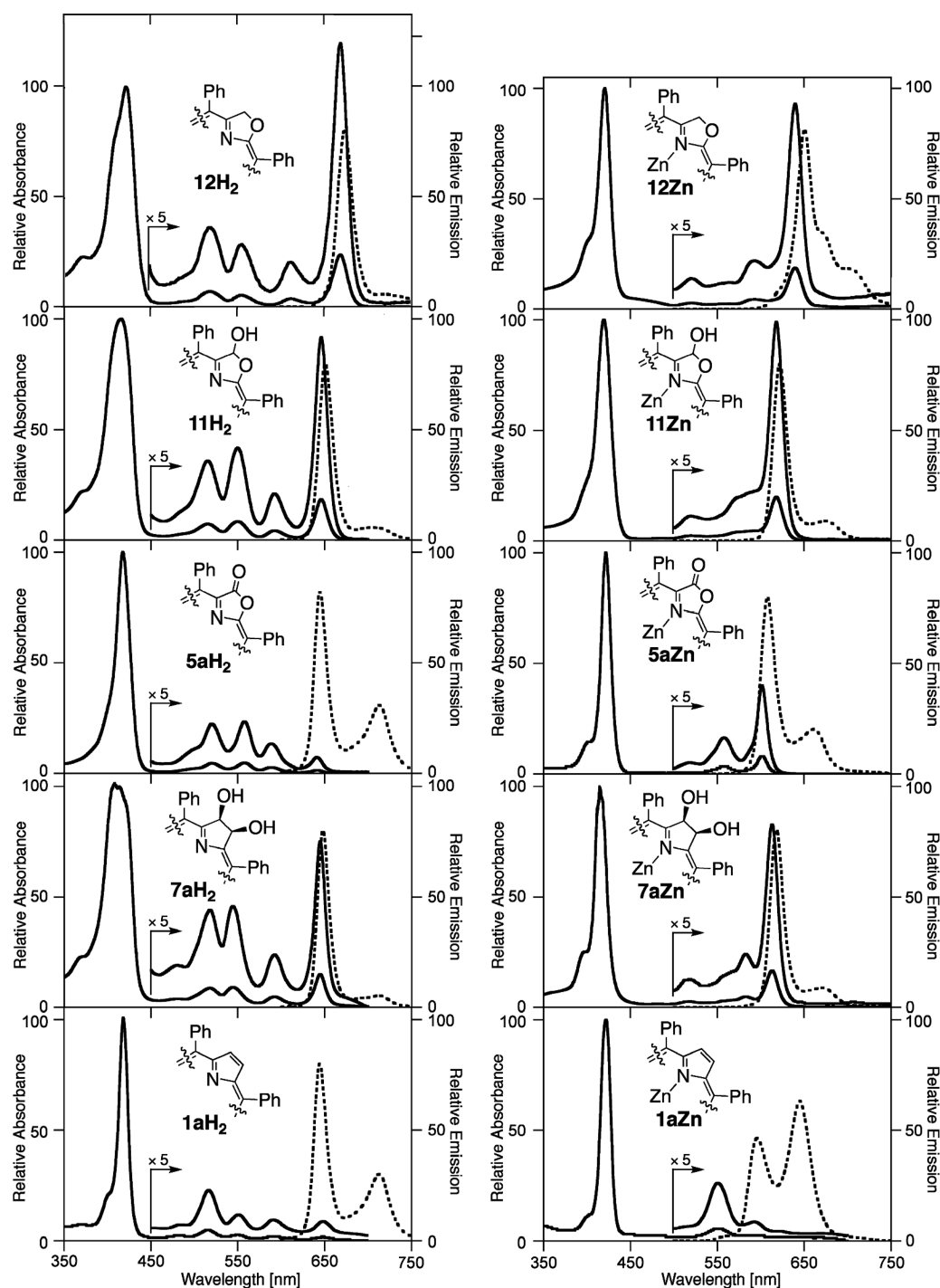


Figure 2. Normalized UV–visible (solid traces) and fluorescence spectra (broken traces) of the compounds indicated (all in CH_2Cl_2 at ambient temperature). Their extinction coefficients are presented in the Experimental Section.

removal of the hydroxy group also results in a significant enhancement of the extinction coefficient of the Q_x band relative to its Soret band. Thus, replacement of the CH_2CH_2 group in chlorins by a CH_2O group has an auxochromic effect, adding to the collection of groups that are known to substantially modify the chlorin chromophore.⁴³ The computations presented below will offer a rationalization for this observation.

Theoretical Analysis of the Free Base Optical Spectra Energies and Intensities. The theoretical studies presented here seek to refine the understanding of the porphyrin-like

optical spectra of porphyrins and the photophysical origins of the unusual intensity and red-shifted transition energy of the Q_x band in 2-oxachlorin **12aH₂**. Because this compound readily oxidizes, we doubted the reliability of the molar extinction coefficient measurements. Thus, the spectra shown in Figure 2 are all relative to a normalized Soret band. This approach is logical, but presents a problem because the SAC–CI and MNDO-PSDCI calculations predict that the intensity of the Soret band, which is made up of two or more transitions, will also change with the modifications. To provide a consistent analysis, we integrated the experimental absorption bands in

energy space to provide oscillator strength ratios. The solvent-averaged results allow a consistent comparison of the calculated and observed values (Table 1).

Table 1. Ratios of the Oscillator Strength of the Q_x Band Divided by the Oscillator Strength of the Soret Band as a Function of Solvent and Comparison to Computed Ratios

$$\left(\frac{f(Q_x)}{f(Q_{\text{Soret}})} \right) \times 10^4$$

solvent	1aH ₂	5aH ₂	7aH ₂	11H ₂	12H ₂
Exp. Average ^a	82	69	230	348	499
SAC-CI ^b	0	120	115	303	377
MNDO-PSDCI ^c	51	21	6	28	117
Dipole Moment (D) ^d	0.0000	5.0056	3.5992	1.3018	1.1781
Dipole Moment* ^e (D) ^c	0.0000	4.7023	0.8262	1.2315	1.3615

^aAverage of the results obtained in 11 solvents (CHCl₃, CH₂Cl₂, DMSO, *n*-hexane, acetone, EtOAc, MeCN, MeOH, THF, pyridine, toluene). For a detailed listing of the solvatochromic properties of 12H₂, see the SI. ^bFrom Figure 3 (left panel). ^cFrom Figure 3 (right panel). ^dB3LYP/6-31G(d) dipole moments computed without the phenyl rings. ^eB3LYP/6-31G(d) dipole moments computed with the phenyl rings.

The results of the high-accuracy (level two) SAC-CI calculations are shown in Figure 3 (left panel). These calculations do not include the phenyl groups, and thus we are observing purely those effects associated with substitutions within the macrocycle. The SAC-CI calculations predict that 12aH₂ will have the most intense Q_x band (Table 1). However, the observed intensity ordering (5aH₂ < 1aH₂ < 7aH₂ < 11H₂ < 12H₂) differs from the SAC-CI predicted intensity ordering (1aH₂ < 7aH₂ < 5aH₂ < 11H₂ < 12H₂) in that 5aH₂ is

calculated to have significantly more Q_x intensity than is observed. An examination of the MNDO-PSDCI calculations, which include the phenyl groups, indicates that the origin of the failure of the SAC-CI calculations on 5aH₂ may be associated with the neglect of the phenyl groups. However, the semiempirical calculations (Figure 3, right panel) underestimate all of the Q_x band intensities, transferring too much oscillator strength into the Q_y bands.

The first and most important observation is that, perhaps contrary to intuition, the dipole moments of the ground state species do not have a significant impact on either the intensities or the red-shifted character of the Q_x bands. The calculated dipole moments, shown in Table 1, correlate with neither the oscillator strengths nor the excitation energies of the bands. Rather, the most red-shifted and most intense Q_x band observed in 2-oxachlorin 12H₂ is observed in a molecule with an intermediate dipole moment of the group studied here.

We examined the configurational characteristics of the Q_x bands and concluded that the key mechanism responsible for both the red shift and the enhanced oscillator strength is mixing of the Q_x band with the low-lying transitions in the Soret region. In the C_{2v} symmetry of chlorin, the Q_x band and the lowest Soret band at ~3.4 eV share the same symmetry (B₂). However, the charge shift upon excitation into the Q_x band decreases the dipole moment of the molecule, a property characteristic of a covalent state (see SI). In contrast, the lowest Soret band (S3) is an “ionic” state, and despite the highly polar environment of the chlorin, these two states do not share configurational space. The insertion of an oxygen atom in place of one of the methylene moieties in the chlorin macrocycle breaks up the symmetry, and has a significant impact on the excitation induced charge shifts (see SI). In particular, all of the excited states are now ionic, and this mixing increases the ground state dipole moment of the molecule. The lowest Q_x band mixes with the S3 Soret transition with an approximately

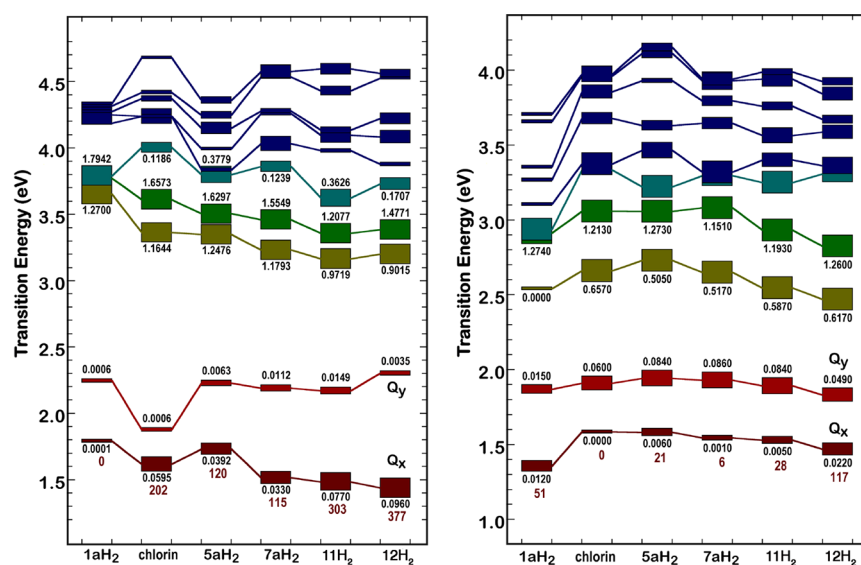


Figure 3. Level ordering of the low-lying electronic transitions of the chromophores investigated. Each electronic transition is represented by a rectangle with vertical position corresponding to the transition energy and height proportional to the oscillator strength. The oscillator strengths for selected transitions are shown in black directly above or below selected transition markers. The red numbers at bottom represent the ratio of the Q_x oscillator strength divided by the total oscillator strength of the Soret bands multiplied by 10^4 ; cf. Table 1. Chlorin refers to the parent 2,3-dihydroporphin structure (C₂₀N₄H₁₆). (Left) Results based on level two SAC-CI molecular orbital theory. These calculations were completed on modified chromophores in which the phenyl groups were replaced by hydrogens. (Right) Results based on MNDO-PSDCI molecular orbital theory. The MNDO-PSDCI calculations were carried out on chromophores that included the phenyl groups.

28% configurational overlap, which transfers oscillator strength from S3 into Q_x . This mixing is visually apparent by reference to Figure 2. Note that the oscillator strength of S3 decreases by an amount comparable to the increase in the oscillator strength of Q_x . Furthermore, the configurational mixing “pushes” these two states apart energetically. Thus, electrostatically induced configurational mixing between S1(Q_x) and S3(Soret) is responsible for both the increased oscillator strength and the increased red shift of the Q_x band.

The MNDO-PSDCI calculations provide insight into the impact of the phenyl groups on the relative properties of the Q_x bands. It is noted that while these semiempirical calculations underestimate the intensities of all the Q_x bands of the chlorins, these calculations do indicate that the Q_x band of oxazolochlorin **12H₂** is significantly more intense than the others, as is observed. The phenyl group near the oxygen atom in this compound rotates slightly to form a weak hydrogen bond between the oxygen atom and the nearby phenyl hydrogen atom (shown in the SI). Upon excitation, this interaction promotes a charge shift that is attributed to an enhanced mixing of Q_x and the S3 state. Thus in the case of **12H₂**, the phenyl groups increase both the red-shift and oscillator strength of Q_x by enhancing the mechanisms responsible for the analogous effects in the compound without phenyl rings.

CONCLUSIONS

We detailed an efficient synthesis of *meso*-tetraarylporpholactones from *meso*-tetraarylporphyrins in two steps using a number of aryl substituents and free base and metallochlorins. We demonstrated this reaction previously for the synthesis of a 21,23-dithiaporpholactone¹⁷ and two porpholactone *N*-oxide isomers.¹⁸ Thus, this methodology can be regarded to be general. In so doing, we have further expanded the synthetic methodologies of converting a porphyrin to pyrrole-modified porphyrins along our “breaking and mending of porphyrins” strategy.

A number of porpholactones (tetraphenylporpholactones **5aH₂** and **5aZn**, diphenylporpholactone **15-II-Zn**) were structurally characterized, displaying their structural relationship to the corresponding porphyrins but also suggest the presence of a steric interaction between the oxazolidone moiety with the flanking phenyl group. The similarity of the optical properties of porphyrins and porpholactones highlight their close electronic relationship.

Replacing a porphyrinoid β,β' -bond by a lactone results in a porphyrin-like optical spectrum for the free base chromophores but more metallochlorin-like properties for the metalloporpholactones. A stepwise reduction of the carbonyl group of **5aH** to an alcohol in porpholactol **11H₂** establishes a chlorin-like spectrum in the free base and zinc(II) complexes. Further reduction of the hemiacetal moiety forms the novel oxazolochlorin chromophore **12H₂**. Compared to porpholactol **11H₂** or 2,3-dihydroxychlorin **7aH₂**, it features a significantly red-shift chlorin-like spectrum with an increased extinction coefficient of the Q_x band. This effect could be traced back by computational analysis to an electrostatically induced configurational mixing between S1(Q_x) and S3(Soret) that is made possible by the desymmetrization of the chromophore upon replacement of the pyrroline moiety in a regular chlorin by an oxazole moiety. X-ray crystal structure analyses of chromophores in all oxidation states showed their planarity, thus providing evidence for the absence of conformational effects in

the modulation of their optical spectra. The presented examples highlight the subtleties that control the structure-electronic properties relationships of porphyrinoids.

The simple syntheses of porpholactones and 2-oxachlorins, their facile derivatization to stable chlorin derivatives potentially bearing many kinds of side chains, and their optical properties are likely to encourage the further study and application of these intriguing chromophores.

EXPERIMENTAL SECTION

Theoretical. Calculations were carried out by using semiempirical MNDO-PSDCI molecular orbital theory^{30,47} as well as SAC-CI theory.⁴⁸ The MNDO-PSDCI calculations used the AM1 Hamiltonian. The configuration interaction included all 64 singles and 2080 doubles generated from the eight highest energy filled and eight lowest energy unfilled π -orbitals. Calculations were carried out with and without phenyl groups for comparative purposes. The SAC-CI calculations were carried out using a full double- ζ D95 basis set,⁴⁹ which has yielded excellent results for large polyatomic chromophores.⁵⁰ Level two integral selection generated a CI basis sets of roughly ~9500 singles and ~600000 doubles. The SAC-CI calculations were carried out on modified structures where hydrogens replaced all of the phenyl groups. All calculations were carried out on structures minimized by using B3LYP/6-31G(d) density functional theory.

X-Ray Single Crystal Diffractometry. X-ray crystallographic analysis: Single crystals of **5aH₂**, **5aZn**, **12H₂**, **13-OMe**, and **15-II-Zn** were coated in either Paratone-N (Exxon) or mineral oil, mounted on a pin and placed a goniometer head under a stream of nitrogen cooled to 100 K. The data were collected on either a Bruker APEX (**5aH₂**, **5aZn**, **12H₂**) or APEX2 (**13-OMe**, and **15-II-Zn**) CCD diffractometer with Mo source K_{α} radiation ($\lambda = 0.71073$). The frames were integrated with the Bruker SAINT software package using a narrow-frame algorithm. Data were corrected for absorption effects using the multiscan method (SADABS) and the structure was solved and refined using the Bruker SHELXTL Software Package until the final anisotropic full-matrix, least-squares refinement of F^2 converged. Data collection and structural parameters for the structure elucidations of **5aH₂**, **5aZn**, **12H₂**, **13-OMe**, and **15-II-Zn** can be found in the SI.

Materials and Instrumentation. *meso*-Tetraarylporphyrins **1H₂** were synthesized according to the method of Adler.⁵¹ The metal complex **1aZn** was prepared from free base *meso*-tetraphenylporphyrin **1aH₂** as described in the literature.⁵²

Flash column chromatography was performed manually in glass columns or on an automated flash chromatography system, on normal-phase silica (solvents used are indicated; isocratic elution modes).

***meso*-Tetrakis(4-*i*-propylphenyl)-cis-2,3-dihydroxychlorin 7bH₂.** Prepared in 31% overall yield (270 mg, 2.93×10^{-4} mol) from *meso*-tetrakis(4-*i*-propyl)phenylporphyrin (**1bH₂**) (1.00 g, 1.12×10^{-3} mol) according to a published general procedure.¹⁶ R_f (silica-CH₂Cl₂) = 0.22, (silica-CH₂Cl₂/1% MeOH) 0.35; ¹H NMR (400 MHz, CDCl₃, δ): 8.67 (d, ³*J* = 4.8 Hz, 2H), 8.50 (s, 2H), 8.33 (d, ³*J* = 4.8 Hz, 2H), 8.07–8.02 (m, 6H), 7.85 (d, 7.36 Hz, 2H), 7.61–7.54 (m, 8H), 6.39 (s, 2H), 3.24–3.17 (m, 6H), 1.52–1.48 (m, 24H), –1.74 (s, 2H, exchangeable with D₂O) ppm; UV–visible (CHCl₃) λ_{\max} (log ϵ) 418 (5.18), 522 (4.20), 548 (4.06) 594 (3.75), 644 (4.40) nm; HR-MS (ESI+, cone voltage = 30 V, 100% CH₃CN, TOF) *m/e* calcd for C₅₆H₅₇N₄O₂ (MH⁺), 817.4482, found 817.4502.

***meso*-Tetrakis(4-trifluoromethylphenyl)-cis-2,3-dihydroxychlorin 7fH₂.** Prepared in 26% overall yield (270 mg, 2.93×10^{-4} mol) from *meso*-tetrakis(4-trifluoromethyl)phenylporphyrin (**1fH₂**) (1.00 g, 1.12×10^{-3} mol) according to a published general procedure.¹⁶ R_f (silica-CH₂Cl₂) = 0.28; ¹H NMR (400 MHz, CDCl₃, δ): 8.62 (d, ³*J* = 4.0 Hz, 2H), 8.43 (s, 2H), 8.30 (d, ³*J* = 4.0 Hz, 2H), 8.27–8.20 (m, 6H), 8.03–7.93 (m, 10H), 6.27 (s, 2H), 3.10 (s, 1H, exchangeable with D₂O), –1.90 (s, 2H, exchangeable with D₂O) ppm; UV–visible (CHCl₃) λ_{\max} (log ϵ) 408 (5.18), 515 (4.12), 542 (4.07) 593 (3.75), 645 (4.39) nm; HR-MS (ESI+, cone voltage =

30 V, 100% CH₃CN, TOF) *m/e* calcd for C₄₈H₂₈F₁₂N₄O₂ (MH⁺) 921.2089, found 921.2128.

meso-Tetrakis(4-methoxyphenyl)-cis-2,3-dihydroxychlorin 7eH₂.²² Prepared in 21% overall yield (220 mg, 2.86 × 10⁻⁴ mol) from *meso*-tetrakis(4-methoxy)phenylporphyrin (**1eH₂**) (1.00 g, 1.36 × 10⁻³ mol) according to a general procedure.¹⁶ *R_f* (silica-CH₂Cl₂/5% MeOH) = 0.49; ¹H NMR (400 MHz, CDCl₃, δ): 8.66 (d, ³J = 4.0 Hz, 1H), 8.50 (s, 1H), 8.33 (d, ³J = 4.0 Hz, 1H), 8.06 (br d, 8.0 Hz 3H), 7.84 (d, 8.0 Hz, 1H), 7.22 (d, 8.0 Hz, 4H), 6.37 (s, 1H), 4.05 (two overlapping s, 6H), 3.21 (s, 1H, exchangeable with D₂O), -1.76 (s, 1H, exchangeable with D₂O) ppm; UV-visible (CHCl₃) λ_{max} (log ε) 418 (5.27), 522 (4.16), 5.51 (4.24), 594 (3.92), 645 (4.38) nm; HR-MS (ESI+, cone voltage = 30 V, 100% CH₃CN, TOF) *m/e* calcd for C₄₈H₄₀N₄O₆ (MH⁺) 769.3021, found 769.2991.

General procedure for the preparation of porpholactones 5 by oxidative diol cleavage of 2,3-dihydroxychlorins 7. To a stirring solution of 7 (0.32 × 10⁻⁴ mol, for **7aH₂** 206 mg) in 25 mL THF was added 18-C-6 (28 mg, 10⁻⁴ mol, 0.33 equiv). KMnO₄ (251 mg, 1.58 mmol, ~5 equiv) was added to the solution, and the mixture was allowed to react for 12 h at ambient temperature, and the reaction monitored by TLC. If needed, additional oxidant was added after 12 h until the starting material was exhausted. The solution was then filtered through a short plug of silica gel or Celite, and the filter cake washed with CH₂Cl₂ until the filtrate was colorless. The combined filtrates were evaporated to dryness by rotary evaporation. The product was purified by column chromatography (silica/CHCl₃), followed by crystallization.

Alternatively, dihydroxy chlorins **7** can be, under the same reaction conditions, reacted with 2–5 equiv of cetyltrimethylammonium permanganate in CH₂Cl₂, followed by the workup described above, also providing excellent yields of **5**.

meso-Tetraphenyl-3-oxo-2-oxaporphyrin (5aH₂). Prepared as crystalline material in 75% isolated yield (150 mg) according to the general procedure from **7aH₂**. Recrystallization from CHCl₃/EtOH. Our IR, UV-vis, LR-MS, ¹H NMR, and analytical data are essentially identical with those reported by Crossley.^{3,53} Supplemented by ¹³C, optical, and HR MS data, they are included here for the purpose of better comparison with the data reported for the reduction products below. *R_f* (silica-CCL₄/CH₂Cl₂ 1:1) = 0.50; ¹H NMR (400 MHz, CDCl₃, δ): 8.80 (dd, ³J = 5.2, ⁴J = 1.5 Hz, 1H), 8.77 (dd, ³J = 4.8, ⁴J = 1.5 Hz, 1H), 8.70 (dd, ³J = 4.8, ⁴J = 1.5 Hz, 1H), 8.60 (d, ³J = 4.6 Hz, 1H), 8.58 (dd, ³J = 5.0, ⁴J = 1.7 Hz, 1H), 8.53 (d, ³J = 4.6 Hz, 1H), 8.10–8.16 (m, 6H), 7.97 (dd, ³J = 7.0, 1.7 Hz, 2H), 7.66–7.78 (m, 12), -1.82 (s, 1H, exchangeable with D₂O), -2.05 (s, 1H, exchangeable with D₂O); ¹³C NMR (100 MHz, CDCl₃, δ): 167.7, 157.1, 154.6, 154.2, 141.6, 141.5, 141.4, 139.4, 138.7, 138.4, 137.6, 137.0, 135.3, 134.5, 134.4, 134.3, 133.8, 132.7, 130.2, 130.1, 128.6, 128.4, 128.3, 128.2, 128.0, 127.9, 127.8, 127.7, 127.2, 127.1, 126.3, 125.7, 121.7, 119.4, 102.9 ppm; UV-vis (CHCl₃) λ_{max} (log ε) 420 (5.56), 522 (4.15), 558 (4.16), 588 (3.95), 640 (3.66); UV-visible (TFA/CHCl₃) λ_{max} 430, 588 (sh), 614; HR-MS (FAB, 3-NBA, quadrupole) *m/e* calcd for C₄₃H₂₈N₄O₂: 632.2212, found 632.2148; Anal. calcd for C₄₃H₂₈N₄O₂: C, 81.63; H, 4.46; N, 8.85%. Found: C, 81.44; H, 4.44; N, 8.80%.

[meso-Tetraphenyl-3-oxo-2-oxaporphyrinato]Zn(II) (5aZn). Prepared either according to the general procedure by oxidation of **7Zn** in 85% isolated yield or, in quantitative yields, by Zn(II)-insertion into **5H₂** using 2 h reflux in CHCl₃/EtOH containing 3 eq Zn(II)(OAc)₂·2H₂O, followed by slow solvent exchange (CHCl₃ to EtOH) on the rotary evaporator. The purple coarse crystals were filtered and air-dried. *R_f* (silica-CH₂Cl₂) = 0.19 or (silica-ethyl acetate/hexane 3:1) = 0.82; ¹H NMR (400 MHz, CDCl₃, δ): 8.75 (d, ³J = 4.5 Hz, 1H), 8.68, 8.67 (two overlapping d, ³J = 4.5 Hz, 2H), 8.63 (d, ³J = 4.5 Hz, 1H), 8.56 (d, ³J = 4.5 Hz, 1H), 8.51 (d, ³J = 4.5 Hz, 1H), 8.11 (d, ³J = 7.8, 2.0 Hz, 4H), 8.06 (dd, ³J = 7.8, 2.0 Hz, 2H), 7.93 (dd, ³J = 7.8, 2.0 Hz, 2H), 7.657.77 (m, 12H); ¹³C NMR (75 MHz, CDCl₃, δ): 173.5, 154.1, 143.4, 142.1, 142.0, 139.0, 138.0, 134.3, 134.0, 133.8, 132.4, 132.3, 132.2, 132.0, 130.9, 130.7, 130.6, 129.5, 128.8, 127.9, 127.8, 127.7, 127.6, 127.5, 126.7, 126.6; UV-visible (CH₂Cl₂) λ_{max} (log ε) 402 (sh), 422 (5.53), 520 (3.54), 558 (4.07), 602 (4.44); LR-

MS (EI, 250 °C) *m/e* 694 (30.9, M⁺), 638 (7.3), 561 (17.4), 483 (3.5), 28 (100); HR-MS (DART⁺, orifice voltage = 30 V, 100% CH₃CN, TOF) *m/e* calcd for C₄₃H₂₇N₄O₂⁶⁴Zn (MH⁺): 695.1425, found 695.1429.

[meso-Tetraphenyl-3-oxo-2-oxaporphyrinato]Ni(II) (5aNi). Prepared in 55% yield (10⁻⁴ mol scale) from **7aNi** according to the general procedure. *R_f* (silica-CH₂Cl₂) = 0.74; ¹H NMR (400 MHz, CDCl₃/10% MeOD, δ): 8.55 (d, ³J = 4.0 Hz, 1H), 8.51–8.47 (two overlapping d, ³J = 4.0 Hz, 2H), 8.45–8.41 (two overlapping d, ³J = 4.0 Hz, 2H), 8.33 (d, ³J = 4.0 Hz, 1H), 7.90–7.85 (m, 6H), 7.74 (m, 2H), 7.66–7.60 (m, 12H). ¹³C NMR (100 MHz, CDCl₃/10% MeOH-d₄, δ): 149.3, 144.9, 144.5, 141.4, 140.9, 139.9, 137.1, 136.0, 133.5, 133.3, 133.0, 131.8, 128.1, 127.7, 127.4, 127.0, 126.9, 124.9, 121.2, 120.3, 100.7; UV-visible (CHCl₂) λ_{max} (log ε) 415 (5.24), 543 (3.96), 586 (4.49) nm; HR-MS (ESI+, cone voltage = 30 V, 100% CH₃CN, TOF) *m/e* calcd for C₄₃H₂₆N₄⁵⁸NiO₂ (M⁺): 688.1409, found: 688.1426.

meso-Tetrakis(4-*i*-propylphenyl)-3-oxo-2-oxaporphyrin (5bH₂). Prepared in 77% yield (13 mg) from **7bH₂** (2.0 × 10⁻⁵ mol, 17 mg) according to the general procedure. *R_f* (silica-CH₂Cl₂) = 0.90; ¹H NMR (400 MHz, CDCl₃, δ): 8.83, 8.81 (two overlapping dd, ³J = 4.5, ⁴J = 1.5 Hz, 2H), 8.74 (dd, ³J = 4.6, ⁴J = 1.3 Hz 1H), 8.63 (d, ³J = 4.5 Hz, 1H), 8.61, 8.59 (dd, ³J = 4.5, ⁴J = 1.5 Hz, 1H), 8.56 (d, ³J = 4.6 Hz, 1H), 8.07–8.02 (m, 6H), 7.90 (d, 8.0 Hz, 2H), 7.60–7.58 (m, 8H), 3.28–3.19 (m, 4H), 1.54–1.50 (m, 24H), -1.62 (s, 1H, exchangeable with D₂O), -2.00 (s, 1H, exchangeable with D₂O) ppm; ¹³C NMR (100 MHz, CDCl₃, δ): 167.6, 156.9, 154.5, 154.1, 148.7, 148.59, 148.57, 148.54, 141.2, 139.3, 138.8, 138.7, 138.6, 136.9, 135.5, 135.0, 134.8, 134.7, 134.4, 134.29, 134.26, 133.5, 132.6, 129.9, 129.8, 127.7, 127.5, 126.0, 125.9, 125.6, 125.5, 125.0, 124.9, 121.5, 119.3, 102.7, 34.11, 34.06, 24.25, 24.19 ppm; UV-visible (CHCl₂) λ_{max} (log ε) 421 (5.46), 523 (4.01), 562 (4.09), 590 (3.81), 642 (3.10) nm; HR-MS (ESI+, cone voltage = 30 V, 100% CH₃CN, TOF) *m/e* calcd for C₅₅H₅₂N₄O₂ (MH⁺) 801.4169, found 801.4149.

meso-Tetrakis(4-*t*-butylphenyl)-3-oxo-2-oxaporphyrin (5cH₂). Prepared in 73% yield (32 mg) from **7cH₂** (5.0 × 10⁻⁵ mol, 43 mg) according to the general procedure. *R_f* (silica-CH₂Cl₂) = 0.89; ¹H NMR (400 MHz, CDCl₃, δ): 8.83 (s, 2H), 8.74 (d, ³J = 4.0 Hz, 1H), 8.63–8.59 (two overlapping d, ³J = 4.0 Hz, 2H), 8.56 (d, ³J = 4.0 Hz, 1H), 8.08–8.04 (m, 6H), 7.92–7.90 (d, 2H), 7.77–7.74 (m, 8H), 3.28–3.19 (m, 4H), 1.60, 1.59, 1.57 (3 s, 36H), -1.62 (s, 1H, exchangeable with D₂O), -1.99 (s, 1H, exchangeable with D₂O) ppm. ¹³C NMR (100 MHz, CDCl₃, δ): 167.6, 156.9, 154.3, 154.0, 151.0, 150.9, 150.8, 150.7, 141.2, 139.3, 138.5, 138.4, 138.3, 136.9, 135.1, 135.0, 134.4, 134.19, 134.09, 134.04, 133.4, 132.3, 129.8, 129.7, 127.7, 127.5, 126.0, 125.4, 124.7, 124.4, 123.9, 123.7, 121.4, 119.3, 102.7, 34.92, 34.91, 34.88, 31.66, 31.62 ppm; UV-visible (CHCl₂) λ_{max} (log ε) 421 (5.44), 523 (4.04), 562 (4.12), 590 (3.87), 642 (3.38) nm; HR-MS (ESI+, cone voltage = 30 V, 100% CH₃CN, TOF) *m/e* calcd for C₅₉H₆₁N₄O₂ (MH⁺) 857.4795, found 857.4787.

meso-Tetrakis(3,4,5-trimethoxyphenyl)-3-oxo-2-oxaporphyrin (5dH₂). Prepared in 95% yield (114 mg) from dihydroxychlorin **7dH₂** (121 mg, 1.2 × 10⁻⁴ mol) according to the general procedure. *R_f* (silica-CH₂Cl₂/5% MeOH) = 0.63; ¹H NMR (400 MHz, CDCl₃, δ): 8.92 (d, ³J = 4.0 Hz, 1H), 8.87–8.83 (m, 2H), 8.72 (d, ³J = 4.0 Hz, 2H), 8.65 (d, ³J = 4.0 Hz, 1H), 7.39 (d, ³J = 8.0 Hz, 2H), 7.30 (s, 1H), 7.18 (s, 1H), 4.16–4.13 (m, 12H), 3.99–3.94 (m, 24H), -1.69 (s, 1H, exchangeable with D₂O), -2.06 (s, 1H, exchangeable with D₂O) ppm; UV-visible (CHCl₂) λ_{max} (log ε) 425 (5.63), 523 (4.32), 561 (4.33), 589 (4.15), 642 (3.82) nm; HR-MS (ESI+, cone voltage = 30 V, 100% CH₃CN, TOF) *m/e* calcd for C₅₅H₅₂N₄O₁₄ (MH⁺) 993.3558, found 993.3528.

[meso-Tetrakis(3,4,5-trimethoxyphenyl)-3-oxo-2-oxaporphyrinato]Ni(II) (5dNi). Prepared in 42% yield (17 mg) from **7dNi** (43 mg, 4.0 × 10⁻⁵ mol) according to the general procedure. *R_f* (silica-CH₂Cl₂/10% MeOH) = 0.73; ¹H NMR (400 MHz, CDCl₃, δ): 8.72 (d, ³J = 4.0 Hz, 1H), 8.69 (d, ³J = 4.0 Hz, 1H), 8.67 (d, ³J = 4.0 Hz, 1H), 8.61 (two overlapping d, ³J = 4.0 Hz, 2H), 8.51 (d, ³J = 4.0 Hz, 1H), 7.20 (s, 4H), 7.13 (s, 2H), 7.01 (s, 2H), 4.11–4.08 (t, 12H), 3.96–3.90 (m, 24H) ppm; ¹³C NMR (100 MHz, CDCl₃, δ): 164.2,

153.2, 152.5, 152.4, 151.9, 151.8, 149.5, 147.4, 145.3, 144.6, 142.1, 141.6, 140.9, 138.2, 138.1, 135.4, 135.3, 134.0, 133.9, 132.2, 131.9, 131.4, 130.9, 130.2, 124.9, 121.2, 120.3, 118.3, 117.8, 111.6, 111.5, 111.4, 110.0, 106.8, 100.8, 61.3, 61.2, 61.00, 56.41, 56.37, 56.28 ppm; UV-visible (CHCl₃) λ_{\max} (log ϵ) 421 (5.18), 545 (3.90), 588 (4.46) nm; HR-MS (ESI+, cone voltage = 30 V, 100% CH₃CN, TOF) *m/e* calcd for C₅₅H₅₀N₄⁵⁸NiO₁₄ (MH⁺) 1048.2677, found 1048.2667.

meso-Tetrakis(4-methoxyphenyl)-3-oxo-2-oxaporphyrin (5eH₂). Prepared in 95% yield (7.8 × 10⁻⁵ mol, 56 mg) from dihydroxychlorin 7eH₂²² (7.8 × 10⁻⁵ mol, 60 mg) according to the general procedure. *R_f* (silica-CH₂Cl₂) = 0.12; ¹H NMR (400 MHz, CDCl₃, δ): 8.80 (dd, ³J = 5.1, ⁴J = 1.4 Hz, 1H), 8.76 (dd, ³J = 5.2, ⁴J = 1.6 Hz, 1H), 8.72 (dd, ³J = 4.8, ⁴J = 1.7 Hz, 1H), 8.61 (d, ³J = 4.7 Hz, 1H), 8.58 (dd, ³J = 4.8 Hz, ⁴J = 1.8 Hz, 1H), 8.53 (d, ³J = 4.6 Hz, 1H), 8.05–8.00 (m, 6H), 7.88 (m, 2H), 7.32–7.24 (m, 8H), 4.04 (s, 12H) –1.59 (s, 1H, exchangeable with D₂O), –1.95 (s, 1H, exchangeable with D₂O) ppm; UV-visible (CHCl₃) λ_{\max} (log ϵ) 425 (5.66), 527 (4.27), 566 (4.38), 590 (4.18), 644 (3.60) nm; HR-MS (ESI+, cone voltage = 30 V, 100% CH₃CN, TOF) *m/e* calcd for C₄₇H₃₆N₄O₆ (MH⁺) 753.2696, found 753.2713.

[meso-Tetrakis(4-methoxyphenyl)-3-oxo-2-oxaporphyrinato]Pd(II) (5ePd). *meso*-Tetrakis(4-methoxyphenyl)-2-oxa-3-oxaporphyrinato 5eH₂ (65.0 mg, 8.63 × 10⁻⁵ mol) was dissolved in PhCN (5 mL) and added to a refluxing solution of PhCN (20 mL) and PdCl₂ (61 mg, 3.44 × 10⁻⁴ mol, 4 equiv) in a round-bottom flask equipped with a magnetic stirring bar and N₂ gas inlet. The mixture was heated to reflux for 3 h.⁵² When the starting material was consumed (reaction control by UV-vis and TLC), the reaction mixture was allowed to cool and was evaporated to dryness by rotary evaporation. The resulting mixture was separated by column chromatography (silica-CH₂Cl₂). The Pd(II) complex was isolated in 71% (50 mg) yield as a magenta powder: *R_f* (silica-CH₂Cl₂) = 0.18; ¹H NMR (400 MHz, CDCl₃, δ): 8.67 (d, ³J = 5.2 Hz, 1H), 8.65 (d, ³J = 4.9 Hz, 1H), 8.64, 8.62, 8.60 (three overlapping d, ³J = 5.0 Hz, 3H), 8.50 (d, ³J = 4.7 Hz, 1H), 7.99–7.94 (m, 6H), 7.83 (dd, ³J = 8.7, ⁴J = 2.2 Hz, 2H), 7.27–7.23 (m, 8H), 4.07 (s, 6H), 4.04 (d, 6H) ppm; UV-vis (CH₂Cl₂) λ_{\max} (log ϵ) 425 (5.34), 500 (3.74), 538 (4.15), 580 (4.60) nm; HR-MS (DART+, orifice voltage = 30 V, 100% CH₃CN, TOF) *m/e* calcd for C₄₇H₃₅N₄O₆Pd(II) ([MH]⁺) 857.1608, found 857.1646.

[meso-Tetrakis(4-methoxyphenyl)-3-oxo-2-oxaporphyrinato]Pt(II) (5ePt). Prepared in good yields (72%, 58 mg) as a red powder as described for the Pd(II) complex from 5eH₂ (65 mg, 8.63 × 10⁻⁵ mol) and PtCl₂ (46 mg, 1.73 × 10⁻⁴ mol, 2.0 equiv). *R_f* (silica-CH₂Cl₂) = 0.17; ¹H NMR (400 MHz, CD₂Cl₂, δ): 8.68–8.62 (m, 5H), 8.50 (d, ³J = 5.1 Hz, 1H), 7.97–7.93 (m, 6H), 7.82 (d, *J* = 6.9, 1.9 Hz, 2H), 7.29–7.22 (m, 8H), 4.03 (d, 7.8 Hz, 12H) ppm; UV-vis (CH₂Cl₂) λ_{\max} (log ϵ) 421 (5.14), 527 (4.07), 568 (4.49) nm; HR-MS (DART+, orifice voltage = 30 V, 100% CH₃CN, TOF) *m/e* calcd for C₄₇H₃₅N₄O₆Pt(II) ([MH]⁺) 946.2208, found 946.2217.

meso-Tetrakis(4-trifluoromethylphenyl)-3-oxo-2-oxaporphyrin (5fH₂). Prepared in 73% yield (8.0 × 10⁻⁵ mol, 73 mg) from dihydroxychlorin 7fH₂ (1.1 × 10⁻⁴ mol, 100 mg) according to the general procedure. *R_f* (silica-CH₂Cl₂) = 0.91; ¹H NMR (400 MHz, CDCl₃, δ): 8.78, 8.76 (two overlapping dd, ³J = 5.0, ⁴J = 1.8 Hz, 2H), 8.67 (dd, ³J = 4.9, ⁴J = 1.9 Hz, 1H), 8.54 (two overlapping d and dd, ³J = 4.6, ⁴J = 2.6 Hz, 2H), 8.47 (d, ³J = 4.7 Hz, 1H), 8.26–8.21 (m, 6H), 8.09–7.99 (m, 10H), –1.70 (s, 1H, exchangeable with D₂O), –2.06 (s, 1H, exchangeable with D₂O) ppm; UV-visible (CH₂Cl₂) λ_{\max} (log ϵ) 416 (5.67), 518 (4.63), 555 (4.35), 588 (4.11), 641 (4.01) nm; HR-MS (ESI+, cone voltage = 30 V, 100% CH₃CN, TOF) *m/e* calcd for C₄₇H₂₄F₁₂N₄O₂²³Na (MNa⁺) 927.1605, found 927.1575.

[meso-Tetrakis(4-trifluoromethylphenyl)-3-oxo-2-oxaporphyrinato]Zn(II) (5fZn). Prepared in near-quantitative yield by zinc(II) insertion into 5fH₂ according to the method described for 5aZn. MW = 968.06 g/mol; *R_f* (silica-CH₂Cl₂) = 0.72; ¹H NMR (300 MHz, CDCl₃, δ): 8.76 (d, ³J = 4.8 Hz, 1H), 8.71 (d, ³J = 4.8 Hz, 1H), 8.68 (m, 2H), 8.61 (d, ³J = 4.6 Hz, 1H), 8.49 (d, ³J = 4.6 Hz, 1H), 8.27 (d, ³J = 7.8 Hz, 4H), 8.22 (d, ³J = 7.9, 2H), 8.04 (m, 8H), 7.97 (d, ³J = 8.1 Hz, 2H) ppm; ¹³C NMR (100 MHz, CDCl₃, δ): 166.2, 154.3,

152.4, 151.9, 151.2, 149.9, 148.1, 147.9, 145.5, 142.4, 141.5, 134.7, 134.3, 134.1, 132.9, 132.8, 132.6, 131.3, 131.1, 131.0, 130.9, 130.6, 130.5, 130.3, 130.1, 126.3, 126.1, 126.0, 125.2, 125.00, 124.97, 124.69, 124.67, 124.20, 124.16, 123.3, 121.0, 119.6, 101.3 ppm; UV-visible (CHCl₃) λ_{\max} (log ϵ): 424 (5.54), 522 (3.64), 560 (4.13), 604 (4.49) nm; Fl λ_{\max} (CHCl₃, λ_{exc} = 424 nm) 607, 660 nm, ϕ = 0.078; HR-MS (ESI+ of MH⁺, 100% CH₃CN, TOF): *m/z* calcd for C₄₇H₂₂F₁₂N₄O₂⁶⁴Zn: 966.0843, found 966.0857.

meso-Tetrakis(pentafluorophenyl)-3-oxo-2-oxaporphyrin (5gH₂). This optimized procedure for the synthesis of this known porpholactone^{4,14,22} is based on the recent availability of the corresponding dihydroxychlorin 7gH₂³⁶ and it is the most efficient method of making this porpholactone reported to date: 5,10,15,20-Tetrakis(pentafluorophenyl)-2,3-dihydroxychlorin 7gH₂ (400 mg, 3.97 × 10⁻⁴ mol) was dissolved in CH₂Cl₂ (150 mL) in a 250 mL round-bottom flask equipped with a stir bar. One equiv of cetyltrimethylammonium permanganate was added every 20 min over a course of 100 min (total addition 800 mg, 1.99 × 10⁻³ mol, 5 equiv). In between additions, the flask was stoppered, shielded from light with aluminum foil, and magnetically stirred at ambient temperature. The disappearance of the starting material/appearance of the product was monitored by TLC. The crude reaction mixture was absorbed onto silica by addition of ~10 g silica gel and evaporation of the solvent by rotary evaporation. The crude material loaded onto silica was purified via column chromatography (24 g silica-CH₂Cl₂/30% hexanes). The red low polarity product was collected and the solvent was removed by rotary evaporation. The product was redissolved in the minimal amount of CHCl₃ and crystallized by slow solvent exchange with EtOH on a rotary evaporator. The bright red product was isolated by filtration and air-dried. Yield: 25–30% (125 mg, 1.26 × 10⁻⁴ mol). Spectroscopic data as reported previously.^{4,14,22}

Alternative procedure using KMnO₄ heterogenized onto silica gel:³³ Either *meso*-tetrakis(pentafluorophenyl)-2,3-dihydroxychlorin osmate ester (0.300 g, 2.16 × 10⁻⁴ mol) or *meso*-tetrakis(pentafluorophenyl)-2,3-dihydroxychlorin 7gH₂ (0.300 g, 2.98 × 10⁻⁴ mol) were dissolved in a 250 mL round-bottom flask equipped with a stir bar in CHCl₃ (100 mL). To the stirred porphyrinoid solution was added KMnO₄ heterogenized onto silica (5.19 g; corresponding to a ~15-fold stoichiometric excess of oxidant). The flask was stoppered, shielded from light with aluminum foil, and stirred at ambient temperature for 24 h. The crude mixture was filtered through Celite to remove the KMnO₄-silica. The resulting solution was evaporated to dryness using rotary evaporation and purified by column chromatography (silica, CH₂Cl₂/70% hexanes) to provide *meso*-tetrakis(pentafluorophenyl)-porpholactone in 10–20% yield. *meso*-Tetrakis(pentafluorophenyl)-2,3-dihydroxychlorin osmate ester was recovered in 85% yield, the chlorin 7gH₂ in 65% yield.

5,15-Diphenylporpholactones 15-I-H₂ and 15-II-H₂. In a 50 mL round-bottom flask shielded from light with aluminum foil, diphenyldihydroxychlorin 14²³ (50 mg, 5.7 × 10⁻⁵ mol) was dissolved in CHCl₃ (20 mL). The solution was stirred magnetically and cetyltrimethylammonium permanganate (CTAP) was added (69 mg, 0.17 mmol, ~3 equiv) at ambient temperature. TLC was used to monitor the formation of a bright pink, nonpolar spot. UV-visible spectroscopy was used to monitor the disappearance of the chlorin peak (at ~650 nm) and the formation of porphyrin-like peaks. The reaction was stirred until the full consumption of 14 was observed (~2 h). The products were then isolated by flash chromatography (silica, CH₂Cl₂), providing an isomeric mixture (approximate ratio 5:1 by ¹H NMR; see ESI) of the diphenylporpholactones in high (~80%) yield. The isomers were separated by preparative TLC (silica-50% petroleum ether 30–60/CHCl₃) but compound 15-I-H₂ could not be isolated in high purity in large enough quantity for its full characterization. For an alternative reaction using the osmate ester of 14, see SI. 15-II-H₂. *R_f* (silica-CH₂Cl₂) = 0.84; ¹H NMR (300 MHz, CDCl₃, δ): 10.10 (s, 1H), 10.03 (s, 1H), 9.34 (dd, ³J = 4.9 Hz, ⁴J = 1.8 Hz, 1H), 9.21 (d, *J* = 4.6 Hz, 1H), 9.09 (d, *J* = 4.5 Hz, 1H), 9.03 (dd, ³J = 4.8 Hz, ⁴J = 1.8 Hz, 1H), 8.96 (d, *J* = 8.0, 4.7 Hz, 1H), 8.85 (d, *J* = 8.0, 4.5 Hz, 1H), 8.18–8.22 (m, 4 H), 7.77–7.85 (m, 6H), –1.99 (s, 1H), –2.58 (s, 1H) ppm; ¹³C NMR (100 MHz, CDCl₃, δ): 170.2, 155.2, 154.9, 154.7,

141.4, 140.8, 137.6, 137.4, 137.0, 136.7, 135.4, 134.7, 134.6, 132.9, 131.8, 131.1, 129.9, 129.0, 128.4, 128.3, 128.25, 127.5, 127.3, 126.35, 124.3, 107.0, 102.6, 101.1 ppm; UV-visible (CHCl_3) λ_{max} (log ϵ): 409 (5.23), 511 (3.92), 549 (4.00), 581 (3.76), 633 (3.81) nm; HR-MS (ESI+, 100% CH_3CN , TOF): m/z calcd for $\text{C}_{31}\text{H}_{21}\text{N}_4\text{O}_2$ (MH^+): 481.1665, found 481.1629.

[5,15-Diphenylporpholactonato]Zn(II) (15-II-Zn). To a stirring solution of 15-II- H_2 (30 mg, 6.3×10^{-5} mol) in CHCl_3 (~5 mL), was added a solution of $\text{Zn}(\text{OAc})_2 \cdot 4 \text{H}_2\text{O}$ in MeOH (27 mg, 1.3×10^{-4} mol, ~2 equiv). The mixture was heated to reflux for ~1 h. TLC was used to monitor the formation of a more polar green product. Upon completion, the solvents were evaporated using rotary evaporation and the product was isolated by column chromatography (silica, 1% MeOH/ CH_2Cl_2) to provide 15-II-Zn in near quantitative yield (33 mg). R_f (silica, 1% MeOH/ CH_2Cl_2) = 0.46; ^1H NMR (300 MHz, CDCl_3 , δ): 9.84 (s, 1H), 9.69 (s, 1H), 9.16 (d, $J = 4.7$ Hz, 1H), 9.08 (d, $J = 4.5$ Hz, 1H), 8.95 (d, $J = 4.3$ Hz, 1H), 8.83–8.87 (m, 3H), 8.08–8.15 (m, 4 H), 7.76–7.79 (m, 6H) ppm; UV-visible (CH_2Cl_2) λ_{max} (log ϵ): 416 (5.81), 514 (3.76), 553 (4.33), 597 (4.79) nm; MS (ESI+, 100% CH_3CN , 30 V cone voltage): $m/z = 543.1$ (MH^+); HR-MS (ESI+ of MH^+ , 100% CH_3CN , TOF): m/z calcd for $\text{C}_{31}\text{H}_{19}\text{N}_4\text{O}_2\text{Zn}$: 543.0799, found 543.0833.

General Procedure for the Preparation of Hemiacetals 11Zn by DIBAL-H Reduction of Lactones 5Zn. Lactone 5Zn (1.4×10^{-4} mol, ~95 mg for 5aZn) were dissolved under an atmosphere of N_2 in dry THF (20–25 mL) and cooled to -78°C . To it was added 20% DIBAL-H (1.0 mL of a 20 wt % solution in hexane, ~7.0 equiv). The reaction mixture stirred for 60 min at this temperature and then allowed to warm to ambient temperature. A noticeable color change from green to blue took place during this time. Once warm, the reaction was quenched by addition of a few drops of water. The solution was then transferred to a separatory funnel, diluted with CH_2Cl_2 (~25 mL), washed twice with 0.1 M aq. HCl, and once with H_2O . The organic layer was collected and dried over anhyd. MgSO_4 . The solution was then evaporated to dryness by rotary evaporation and used as is or purified by preparative plate or column chromatography (Note: Care should be taken not to expose the hemiacetal 9Zn to any alcohols or the corresponding acetal 10Zn will be isolated).

[meso-Tetraphenyl-3-hydroxy-2-oxachlorinato]Zn(II) (11Zn). Prepared as a purple powder in 80–90% isolated yields (180 mg) from porpholactol zinc complex 5aZn (200 mg, 0.287 mmol) according to the general procedure. R_f (silica- CH_2Cl_2) = 0.06; ^1H NMR (400 MHz, CDCl_3 , δ): 8.61 (d, $^3J = 4.4$ Hz, 1H), 8.52 (d, $^3J = 4.2$ Hz, 1H), 8.42 (d, $^3J = 4.0$ Hz, 1H), 8.38 (d, $^3J = 4.4$ Hz, 1H), 8.34 (d, $^3J = 4.0$ Hz, 1H), 8.20 (brs, 1H), 8.12 (m, 2H), 8.04 (m, 2H), 7.73 (m, 8H), 7.50 (m, 9H), 7.26 (s, 1H), 3.02 (s, 1H) ppm; ^{13}C NMR (100 MHz, CDCl_3 , δ): 190.7, 162.7, 187.3, 157.7, 153.9, 149.6, 145.3, 143.2, 140.6, 140.3, 139.3, 138.0, 137.2, 136.7, 136.6, 136.2, 135.0, 133.8, 133.2, 131.9, 129.2, 129.1, 128.5, 128.4, 128.3, 127.6, 127.4, 127.3, 126.2, 125.9, 125.7, 124.2, 121.6, 112.1 ppm; UV-visible (CH_2Cl_2) λ_{max} (log ϵ): 415 (5.37), 453 (3.87), 513 (3.75), 538 (3.70), 580 (3.97), 615 (4.60), 795 (3.37) nm; Fl (CH_2Cl_2 , $\lambda_{\text{excitation}} = 420$ nm) λ_{max} : 621, 672 nm; HR-MS (FAB+ of M^+ , PEG, quadrupole): m/z calcd for $\text{C}_{43}\text{H}_{28}\text{O}_2\text{N}_4$: 696.1504, found 696.1519.

meso-Tetraphenyl-3-hydroxy-2-oxachlorins (11H₂). Prepared in >90% yields (up to 500 mg scale) by demetalation of 11Zn. The dilute HCl wash in the general procedure for the preparation of 11Zn was replaced with a wash of half-concentrated aqueous HCl, followed by several washes with H_2O saturated aq. Na_2CO_3 solution, and again H_2O . The organic layer was dried over anhyd. MgSO_4 , evaporated to dryness and purified by preparative plate or column chromatography (Note: Care should be taken not to expose the hemiacetal 11H₂ to any alcohols or the corresponding acetals 13H₂ will be isolated). R_f (silica- CH_2Cl_2) = 0.54; ^1H NMR (400 MHz, CDCl_3 , δ): 8.58 (d, $^3J = 4.5$ Hz, 1H), 8.50 (d, $^3J = 4.5$ Hz, 1H), 8.42 (t, $^3J = 4.5$ Hz, 3.51, 2H), 8.34 (d, $^3J = 4.0$ Hz, 1H), 8.17 (d, $^3J = 4.5$ Hz, 1H), 8.10 (m, 5H), 7.87 (t, $^3J = 5.8$ Hz, 7.77, 2H), 7.71 (brs, 13H), 3.83 (d, $^3J = 7.2$ Hz, 1H), -0.76 (s, 1H), -1.13 (s, 1H) ppm; ^{13}C NMR (100 MHz, CDCl_3 , δ): 164.3, 155.1, 152.0, 151.6, 142.0, 136.9, 135.1, 134.1,

133.9, 133.7, 131.9, 131.5, 129.9, 128.2, 128.2, 128.1, 128.0, 127.9, 127.7, 127.1, 127.0, 125.3, 122.1, 112.2, 100.2 ppm; UV-vis (CH_2Cl_2) λ_{max} (log ϵ): 416 (5.26), 515 (4.11), 550 (4.18), 592 (3.87), 646 (4.51) nm; Fl (CH_2Cl_2 , $\lambda_{\text{excitation}} = 420$ nm) λ_{max} : 651, 704 nm; +ESI-MS (cone voltage 70 V, 100% CH_3CN): $m/z = 635$ (MH^+); HR-MS (FAB+ of MH^+ , PEG, quadrupole): m/z calcd for $\text{C}_{43}\text{H}_{31}\text{O}_2\text{N}_4$: 635.2447, found 635.2435; Anal. calcd for $\text{C}_{43}\text{H}_{30}\text{N}_4\text{O}_2$: C, 81.37; H, 4.76; N, 8.83%. Found: C, 80.72; H, 4.94; N, 8.70%.

meso-Tetraphenyl-2-oxachlorin (12H₂). To 11H₂ (30 mg, 4.8×10^{-2} mmol) dissolved in dry CH_2Cl_2 under N_2 and stirred at room temperature was added excess Et_3SiH (125 μL , 16 equiv) and excess $\text{BF}_3 \cdot \text{OEt}_2$ (250 μL , 30 equiv). The reaction proceeded for 10 min. The reaction can also be catalyzed by Amberlyst 15 (600 mg) but then takes 12 h for completion. The solution was then washed twice with a concd. aq. NaHCO_3 solution, dried over anhyd. MgSO_4 , and evaporated to dryness by rotary evaporation. Flash chromatography (silica/ CH_2Cl_2) was used to isolate and purify the product. It was precipitated by slow solvent exchange with cyclohexane to produce 12H₂ as a purple powder in near-quantitative yields. The product undergoes spontaneous (photo)oxidations over time. R_f (silica- CH_2Cl_2) = 0.98; ^1H NMR (400 MHz, CDCl_3 , δ): 8.43 (dd, $^3J = 5.0$, $^4J = 1.6$ Hz, 1H), 8.38 (dd, $^3J = 4.8$, $^4J = 1.8$ Hz, 1H), 8.28 (d, $^3J = 4.4$ Hz, 1H), 8.22 (dd, $^3J = 5.0$, $^4J = 1.8$ Hz, 1H), 8.20 (d, $^3J = 4.4$ Hz, 1H), 8.07 (m, 4H), 7.98 (m, 3H), 7.83 (dd, $^3J = 7.8$, $^4J = 1.6$ Hz, 2H), 7.69 (m, 12H), 6.54 (s, 2H), 0.15 (s, 1H), -0.25 (s, 1H) ppm; ^{13}C NMR (100 MHz, CDCl_3 , δ): 170.1, 156.0, 154.5, 151.6, 144.0, 142.0, 133.9, 133.8, 133.7, 132.8, 131.9, 131.2, 130.0, 129.0, 128.3, 128.2, 128.1, 128.0, 127.9, 127.7, 127.1, 127.0, 124.2, 107.9, 99.0, 76.4 ppm; UV-vis (CH_2Cl_2) λ_{max} (rel. intensity): 373 (shoulder), 422 (1.00), 519 (0.07), 554 (0.06), 612 (0.04), 668 (0.26) nm; Fl (CH_2Cl_2 , $\lambda_{\text{excitation}} = 420$ nm) λ_{max} : 674, 732 (sh) nm; HR-MS (ESI+, 100% CH_3CN , TOF) expected for $\text{C}_{43}\text{H}_{31}\text{N}_4\text{O}$ (MH^+): 619.2492, found 619.2477.

[meso-Tetraphenyl-2-oxachlorinato]Zn(II) (12Zn). To 12H₂ (30 mg, 4.8×10^{-2} mmol) dissolved in dry CH_2Cl_2 in DMF was added $\text{Zn}(\text{OAc})_2 \cdot 2\text{H}_2\text{O}$ (2 equiv). The solution was warmed to 80°C and metalation was monitored by TLC. Upon completion, the solution was evaporated to dryness under high vacuum. The residue was dissolved in CH_2Cl_2 , and flash chromatography (silica- CH_2Cl_2) was used to separate the product. The product was evaporated to dryness to yield a green-purple product in 90% yield. The product undergoes spontaneous (photo)oxidations. ^1H NMR (400 MHz, CDCl_3 , δ): 8.31 (d, $^3J = 4.8$ Hz, 1H), 8.29 (d, $^3J = 4.6$ Hz, 1H), 8.17 (d, $J = 4.5$ Hz, 1H), 8.09 (d, $^3J = 4.5$ Hz, 1H), 8.07 (d, $^3J = 4.8$ Hz, 1H), 7.97–8.01 (m, 3H), 7.89 (m, 2H), 7.87 (m, 1H), 7.86 (d, $^3J = 4.5$ Hz, 1H), 7.77 (dd, $J = 7.8$, 1.6 Hz, 2H), 7.62–7.67 (m, 12H), 6.54 (s, 2H) ppm; UV-vis (CH_2Cl_2) λ_{max} (rel. intensity): 420 (1.00), 520 (0.02), 591 (0.04), 640 (0.19); Fl (CH_2Cl_2 , $\lambda_{\text{excitation}} = 420$ nm) λ_{max} : 651, 670, 699 nm; HR-MS (ESI+, 100% CH_3CN , TOF) expected for $\text{C}_{43}\text{H}_{29}\text{N}_4\text{O}^{65}\text{Zn}$ (MH^+): 681.1627, found 681.1619.

General Procedure for the Conversion of Hemiacetals 11 to MeO-based Acetals 13. Excess MeOH was added to a stirring solution of 11H₂ or 11Zn in CH_2Cl_2 . Traces of TFA vapors (from a TFA bottle head space, delivered via pipet) were added, and the reaction was monitored by TLC for completion. The acid was then neutralized with Et_3N (1 drop), the solution washed, dried over anhyd. MgSO_4 , evaporated to dryness, and purified by column or preparative plate chromatography.

[meso-Tetraphenyl-3-methoxy-2-oxachlorinato]Zn(II) (13-OMeZn). Prepared according to the general procedure from 11aZn and MeOH in 85% yields: R_f (silica- CH_2Cl_2) = 0.54; ^1H NMR (400 MHz, CDCl_3) δ 3.32 (s, 3H), 7.56 (s, 1H), 7.66 (m, 12 H), 7.82 (m, 1H), 7.87 (brs, 1H), 8.00 (m, 3H), 8.10 (m, 3H), 8.12 (d, $^3J = 4.6$ Hz, 1H), 8.31 (d, $^3J = 4.4$ Hz, 1H), 8.34 (d, $^3J = 4.6$ Hz, 1H), 8.38 (d, $^3J = 4.4$ Hz, 1H), 8.48 (d, $^3J = 4.4$ Hz, 1H), 8.52 (d, $^3J = 4.6$ Hz, 1H) ppm; ^{13}C NMR (100 MHz, CDCl_3) δ 162.8, 156.2, 154.5, 146.8, 142.6, 139.6, 134.7, 134.3, 134.0, 134.0, 133.8, 131.5, 130.6, 128.7, 128.0, 128.0, 127.9, 127.6, 127.6, 127.2, 127.1, 126.2, 123.4, 113.6, 106.5, 99.4, 55.2 ppm; UV-vis (CH_2Cl_2) λ_{max} (log ϵ): 419 (5.23), 519 (3.60), 572 (shoulder), 618 (4.53) nm; Fl (CH_2Cl_2 , $\lambda_{\text{excitation}} = 420$

nm) λ_{\max} : 621, 675 nm; HR-MS (FAB+ of M^+ , PEG, quadrupole): m/z calc'd for $C_{44}H_{30}O_2N_4$: 710.1660, found 710.1673.

meso-Tetraphenyl-3-isopropoxy-2-oxachlorin (13-OⁱPr). General Procedure for the Conversion of Hemiacetals 11 to Acetals 13. Isopropanol (1 mL) was added to a stirring solution of 11H₂ (11.5 mg, 1.9×10^{-5} mol) in $CHCl_3$ (3 mL) at room temperature. Traces of TFA vapors (from a TFA bottle head space, delivered via pipet) were added, and the reaction was monitored by TLC. The reaction was complete within 3 h. Upon completion, the acid was neutralized with Et_3N (1 drop), the solution washed, dried over anhydrous $MgSO_4$, evaporated to dryness using rotary evaporation, and purified by flash column chromatography (DCM) or preparative plate. Yield > 95% (12 mg). R_f (silica- CH_2Cl_2) = 0.96; 1H NMR (300 MHz, $CDCl_3$, δ): 8.60 (d, $^3J = 4.2$ Hz, 1H), 8.51 (d, $^3J = 4.2$ Hz, 1H), 8.47 (d, $^3J = 4.2$ Hz, 1H), 8.43 (d, $^3J = 4.2$ Hz, 1H), 8.35 (d, $^3J = 4.2$ Hz, 1H), 8.04–8.19 (m, 7H), 7.89 (br, 1H), 7.66–7.73 (m, 14H), 3.96 (m, 1 H), 1.27 (d, $^3J = 6.0$ Hz, 3H), 0.91 (d, $^3J = 6.0$ Hz, 3H), –0.73 (s, 1H), –1.09 (s, 1H) ppm; UV-vis (CH_2Cl_2) λ_{\max} (log ϵ): 418 (5.38), 516 (4.21), 550 (4.26), 593 (3.97), 647 (4.63) nm; LR-MS (ESI+, 100% CH_3CN , 30 V cone voltage, TOF): m/z 677.1 (MH^+), 634.7 ($MH^+ - C_3H_7$); HR-MS (ESI+ of M^+ , 100% CH_3CN): m/z calc'd for $C_{46}H_{36}N_4O_2$: 677.2917, found 677.3018.

meso-Tetraphenyl-3-methoxy-2-oxachlorin (13-OMe). Prepared according to the general procedure from 11H₂ (10 mg, 0.016 mmol) and methanol (1 mL) in near-quantitative yield. Spectroscopic properties as described previously.⁸

meso-Tetraphenyl-3-cyclohexanoxy-2-oxachlorin (13-O^{Hex}). Prepared according to the general procedure from 11H₂ (10 mg, 0.016 mmol) and cyclohexanol (1 mL) in >95% isolated yields (11 mg): R_f (silica- CH_2Cl_2) = 0.98; 1H NMR (300 MHz, $CDCl_3$, δ): 8.59 (dd, $^3J = 4.9$, $^4J = 1.5$ Hz, 1H), 8.51 (dd, $^3J = 3.8$, $^4J = 1.7$ Hz, 1H), 8.46 (dd, $^3J = 4.9$, $^4J = 1.7$ Hz, 1H), 8.43 (d, $^3J = 4.5$ Hz, 1H), 8.35 (d, $^3J = 4.5$ Hz, 1H), 7.88–8.19 (m, 8H), 7.69–7.72 (m, 13H), 3.59–3.66 (m, 1H), 0.89–1.72 (m, 10H), –0.71 (s, 1H), –1.08 (s, 1H) ppm; ^{13}C NMR (100 MHz, $CDCl_3$, δ): 165.5, 154.9, 151.8, 151.4, 142.9, 142.1, 142.0, 141.1, 140.1, 139.1, 136.7, 135.3, 134.5, 134.0, 133.9, 131.7, 131.1, 129.7, 127.9, 127.85, 127.8, 127.7, 127.6, 127.5, 127.0, 126.9, 125.9, 125.0, 121.9, 121.3, 112.2, 105.1, 100.4, 79.4, 33.7, 31.9, 25.8, 24.1 ppm; UV-visible (CH_2Cl_2) λ_{\max} (log ϵ): 418 (5.31), 516 (4.14), 550 (4.19), 594 (3.88), 647 (4.55) nm; HR-MS (ESI+ of M^+ , 100% CH_3CN , TOF): m/z calc'd for $C_{49}H_{41}N_4O_2$: 717.3230, found 717.3212.

meso-Tetraphenyl-3-tert-butoxy-2-oxachlorin (13-O^tBu). Prepared according to the general procedure from 11H₂ (12 mg, 0.019 mmol) and *tert*-butanol (1 mL) in 80% isolated yield (9.8 mg): R_f (silica- CH_2Cl_2) = 0.92; 1H NMR (300 MHz, $CDCl_3$, δ): 8.58 (d, $^3J = 4.7$ Hz, 1H), 8.44–8.49 (m, 2H), 8.41 (d, $^3J = 4.5$ Hz, 1H), 8.34 (d, $^3J = 4.5$ Hz, 1H), 8.03–8.19 (m, 8H), 7.84–7.89 (m, 2H), 7.63–7.72 (m, 12H), 1.09 (s, 9H), –0.71 (s, 1H), –1.07 (s, 1H) ppm; ^{13}C NMR (100 MHz, $CDCl_3$, δ): 165.3, 154.8, 152.1, 151.7, 142.9, 142.2, 142.1, 142.0, 141.2, 140.4, 139.1, 136.7, 135.5, 134.4, 134.3, 134.1, 134.0, 133.9, 133.3, 131.6, 131.4, 129.6, 128.0, 127.96, 127.92, 127.8, 127.7, 127.6, 127.54, 127.51, 127.0, 126.9, 125.9, 125.0, 121.7, 121.2, 112.0, 105.8, 100.6, 100.4, 64.8, 28.5 ppm; UV-visible (CH_2Cl_2) λ_{\max} (log ϵ): 418 (5.20), 514 (4.05), 550 (4.08), 594 (3.79), 647 (4.46) nm; HR-MS (DART+, 20 V orifice voltage, 100% CH_3CN , TOF): m/z calc'd for $C_{47}H_{39}N_4O_2$ (MH^+): 691.3037, found 691.3056.

[meso-Tetraphenyl-3-octoxy-2-oxachlorin] (13-OⁿOct). Prepared according to the general procedure from 11H₂ (10 mg, 0.016 mmol) and *n*-octanol (1 mL) in 92% isolated yield (11.4 mg): R_f (silica- CH_2Cl_2) = 0.92; 1H NMR (300 MHz, $CDCl_3$, δ): 8.59 (dd, $^3J = 4.5$, $^4J = 1.5$ Hz, 1H), 8.52 (dd, $^3J = 4.6$, $^4J = 1.7$ Hz, 1H), 8.45 (dd, $^3J = 5.8$, $^4J = 1.7$ Hz, 1H), 8.43 (d, $^3J = 4.6$ Hz, 1H), 8.35 (d, $^3J = 4.5$ Hz, 1H), 8.21 (dd, $^3J = 5.8$, $^4J = 1.7$ Hz, 1H), 7.85–8.18 (m, 8H), 7.64–7.77 (m, 12H), 7.59 (s, 1H), 3.64–3.67 (m, 1H), 3.42–3.45 (m, 1H), 1.24–1.28 (m, 17H), –0.73 (s, 1H), –1.09 (s, 1H) ppm; ^{13}C NMR (100 MHz, $CDCl_3$) δ 165.0, 154.9, 151.9, 151.0, 143.0, 142.1, 142.0, 140.9, 139.9, 139.0, 136.8, 135.0, 134.5, 134.2, 134.1, 134.0, 133.9, 133.5, 131.8, 131.2, 129.7, 128.1, 128.0, 127.9, 127.8, 127.7, 127.6, 127.65, 127.0, 126.9, 125.9, 125.1, 121.9, 121.4, 112.2, 105.9,

100.3, 69.4, 32.0, 29.9, 29.5, 29.4, 26.3, 22.9, 14.3 ppm; UV-visible (CH_2Cl_2) λ_{\max} (log ϵ): 417 (5.23), 515 (4.06), 550 (4.11), 593 (3.79), 646 (4.48) nm; HR-MS (ESI+ of M^+ , 100% CH_3CN , TOF): m/z calc'd for $C_{51}H_{47}N_4O_2$: 747.3699, found 747.3705.

meso-Tetraphenyl-3-(+)cholesteroxy-2-oxachlorin (13-O-Chol). Prepared according to the general procedure from 11H₂ (33.9 mg, 0.053 mmol) and cholesterol (20.7 mg, 2 equiv) in 88% isolated yield (47 mg): R_f (silica- CH_2Cl_2) = 0.96; 1H NMR (300 MHz, $CDCl_3$, δ): 8.63 (d, $^3J = 4.8$ Hz, 1H), 8.55 (m, 1H), 8.51 (d, $^3J = 1.5$ Hz, 1H), 8.47 (d, $^3J = 4.5$ Hz, 1H), 8.39 (d, $^3J = 4.5$ Hz, 1H), 8.10–8.25 (m, 8H), 7.9 (d, $^3J = 0.3$ Hz, 2H), 7.66–7.76 (m, 13H), 5.29–5.36 (m, 1H), 3.55–3.63 (m, 1H), 2.32–2.64 (m, 1H), 2.12–1.72 (m, 6H), 1.28–1.62 (m, 15H), 0.99–1.22 (m, 12H), 0.96 (s, 3H), 0.98 (s, 3H), 0.71 (s, 3H), –0.74 (s, 1H), –1.06 (s, 1H) ppm; ^{13}C NMR (100 MHz, $CDCl_3$, δ): 165.1, 165.0, 155.0, 154.9, 151.9, 151.2, 151.1, 143.0, 142.2, 142.1, 141.2, 141.1, 141.0, 140.2, 140.1, 139.1, 139.0, 136.8, 136.7, 135.4, 135.3, 134.6, 134.2, 134.1, 134.0, 133.5, 131.8, 131.1, 131.0, 129.8, 128.2, 128.1, 128.0, 127.9, 127.8, 127.7, 127.6, 127.1, 126.9, 126.0, 125.1, 125.1, 122.1, 122.0, 122.0, 121.9, 121.4, 121.4, 112.2, 105.3, 105.2, 100.5, 100.4, 81.1, 81.0, 57.0, 56.4, 50.3, 42.6, 40.8, 40.0, 39.8, 38.6, 37.6, 37.4, 36.9, 36.8, 36.5, 36.1, 32.3, 32.2, 32.1, 30.1, 28.5, 28.3, 28.2, 24.6, 24.1, 23.1, 22.9, 21.4, 21.3, 19.6, 19.0, 12.1 ppm; UV-visible (CH_2Cl_2) λ_{\max} (log ϵ): 419 (5.24), 515 (4.16), 552 (4.18), 594 (3.95), 655 (3.79) nm; HR-MS (ESI+, 100% CH_3CN , TOF): m/z calc'd for $C_{70}H_{75}N_4O_2$ (MH^+): 1003.5890, found 1003.5893.

meso-Tetraphenyl-3-pregnenolonoxy-2-oxachlorin (13-O-Preg). Prepared according to the general procedure from 11H₂ (33.5 mg, 0.053 mmol) and pregnenolone (33.4 mg, 2 equiv) in 83% isolated yield (41 mg): R_f (silica- CH_2Cl_2) = 0.55; 1H NMR (300 MHz, $CDCl_3$, δ): 8.61 (d, $^3J = 4.5$ Hz, 1H), 8.53 (d, $^3J = 4.5$ Hz, 1H), 8.47 (t, $^3J = 4.5$ Hz, 1H), 8.44 (d, $^3J = 4.5$ Hz, 1H), 8.36 (d, $^3J = 4.5$ Hz, 1H), 7.89–8.22 (m, 9H), 7.65–7.74 (m, 13H), 5.30 (dd, $^3J = 23.3$ Hz, 4.5 Hz, 1H), 3.55–3.61 (m, 1H), 2.29–2.62 (m, 2H), 2.20 (m, 1H), 2.14 (s, 3H), 2.02–2.013 (m, 3H), 1.04–1.94 (m, 14H), 0.96 (s, 3H), 0.63 (s, 3H), –0.74 (s, 1H), –1.08 (s, 1H) ppm; ^{13}C NMR (100 MHz, $CDCl_3$) δ 209.8, 151.9, 142.9, 142.1, 142.0, 141.1, 141.1, 141.0, 140.9, 136.8, 136.7, 135.4, 135.3, 134.5, 134.2, 134.1, 134.0, 133.5, 131.8, 131.1, 131.0, 129.8, 128.2, 128.1, 128.0, 127.9, 127.8, 127.7, 127.1, 126.9, 126.0, 125.1, 125.0, 122.0, 121.9, 121.7, 121.6, 112.2, 105.3, 105.2, 100.4, 80.9, 80.7, 63.9, 57.1, 50.1, 44.2, 40.7, 39.0, 38.5, 37.5, 37.4, 36.9, 36.8, 32.1, 31.8, 30.0, 28.1, 24.7, 23.0, 21.3, 21.2, 19.6, 19.5, 13.4 ppm; UV-visible (CH_2Cl_2) λ_{\max} (log ϵ): 419 (5.28), 517 (4.13), 550 (4.17), 593 (3.88), 647 (4.52) nm; HR-MS (ESI+, 100% CH_3CN , TOF): m/z calc'd for $C_{64}H_{61}N_4O_3$ (MH^+): 933.4744, found 933.4733.

meso-Tetraphenyl-3-ethioxy-2-oxachlorin (13-SEt). General Procedure for the Conversion of Hemiacetals 11H₂ to RS-based Thiaacetals 13-SR. Excess ethanethiol (1 to 2 mL) was added to a stirring solution of 11H₂ (10 mg, 0.015 mmol) in $CHCl_3$ (3–5 mL) at room temperature. Traces of TFA vapors (from a TFA bottle head space, delivered via pipet) were added, and the reaction was monitored by TLC. The reaction was complete within 3–5 h. Upon completion, the acid was neutralized with Et_3N (1 drop), the solution washed, dried over anhydrous $MgSO_4$, evaporated to dryness using rotary evaporation, and purified by silica gel flash column or preparative plate chromatography (CH_2Cl_2). Isolated yield 90% (9.6 mg): R_f (silica- CH_2Cl_2) = 0.96; 1H NMR (300 MHz, $CDCl_3$, δ): 8.50–8.52 (m, 1H), 8.43–8.44 (m, 1H), 8.33–8.35 (m, 2H), 8.26–8.27 (m, 1H), 7.99 (m, 8H), 7.90–7.91 (m, 1H), 7.67–7.80 (m, 12H), 2.31–2.41 (m, 1H), 2.12–2.19 (m, 1H), 0.89–0.93 (m, 3H), –0.30 (s, 1H), –0.65 (s, 1H) ppm; ^{13}C NMR (100 MHz, $CDCl_3$, δ): 165.9, 154.9, 153.1, 151.9, 143.4, 141.9, 141.8, 141.4, 139.9, 138.7, 136.8, 135.5, 134.6, 134.1, 133.9, 133.8, 133.3, 131.6, 131.1, 129.9, 128.5, 128.2, 128.0, 127.92, 127.94, 127.97, 127.8, 127.7, 127.1, 126.95, 126.9, 126.3, 124.9, 121.8, 110.6, 100.1, 90.8 ppm; UV-visible (CH_2Cl_2) λ_{\max} (log ϵ): 420 (5.31), 457 (4.43), 518 (4.13), 555 (4.07), 608 (3.88), 660 (4.51) nm; LR-MS (ESI+, 100% CH_3CN , 30 V cone voltage): m/z 679.1 (MH^+), upon exposure to ambient light and environment, significant peak of 695.7 (MHO^+) is observed; HR-MS

(ESI+, 100% CH₃CN, TOF): *m/z* calcd for C₄₅H₃₅N₄O₅ (MH⁺): 679.2532, found 679.2471.

meso-Tetraphenyl-3-hexanethioxy-2-oxachlorin (13-SⁿHex). Prepared according to the general procedure from 11H₂ (10 mg 0.014 mmol) and hexanethiol (1 mL) in 50% isolated yield (5.8 mg): *R_f* (silica – CH₂Cl₂) = 0.92; ¹H NMR (300 MHz, CDCl₃, δ): 8.50–8.51 (m, 1H), 8.42–8.43 (m, 1H), 8.33–8.34 (m, 2H), 8.26–8.27 (m, 1H), 7.98–8.23 (m, 8H), 7.89–7.91 (m, 1H), 7.65–7.75 (m, 13H), 2.35–2.42 (m, 1H), 2.15–2.18 (m, 1H), 0.71–1.28 (m, 13H), –0.30 (s, 1H), –0.65 (s, 1H) ppm; UV–visible (CH₂Cl₂) λ_{max} (log ε): 422 (5.17), 518 (3.99), 553 (3.93), 603 (3.65), 659 (4.35) nm; HR-MS (ESI+, 100% CH₃CN, TOF): *m/z* calcd for C₄₉H₄₃N₄O₅ (MH⁺): 735.3153, found 735.3097.

meso-Tetraphenyl-3-N-morpholinyl-2-oxachlorin (13-N^{morph}). General procedure for the conversion of hemiacetals 11 to amins. A small-scale Soxhlet containing 3 Å molecular sieves was attached to a 50 mL round-bottom flask. Excess amine (5 to 10 equiv) was then added to a stirring solution of 11H₂ (30 mg, 0.043 mmol) in benzene (10–15 mL). A few drops of TFA were added and the mixture was refluxed for several days (3–5 days). The reaction progress was monitored by TLC and upon completion, the acid was neutralized with Et₃N (1 drop), dried over anhydrous MgSO₄, evaporated to dryness using rotary evaporation, and purified by flash column chromatography (CH₂Cl₂) or preparative plate to give 13-N^{morph} in 30% isolated yield (9 mg): *R_f* (silica–CH₂Cl₂) = 0.60; ¹H NMR (300 MHz, CDCl₃, δ): 8.52–8.54 (m, 1H), 8.45–8.47 (m, 1H), 8.36–8.37 (m, 2H), 8.28–8.29 (m, 1H), 7.84–8.15 (m, 10H), 7.64–7.70 (m, 11H), 7.44 (s, 1H), 3.47–3.48 (m, 2H), 3.29–3.30 (m, 2H), 2.58–2.59 (m, 2H), 2.38–2.43 (m, 2H), –0.44 (s, 1H), –0.86 (s, 1H) ppm; ¹³C NMR (100 MHz, CDCl₃, δ): 166.5, 154.9, 151.6, 150.6, 143.4, 142.0, 141.9, 141.2, 140.5, 139.2, 136.8, 135.2, 134.2, 134.0, 133.9, 133.8, 133.3, 131.5, 130.1, 129.7, 128.1, 128.0, 127.9, 127.8, 127.7, 127.6, 127.2, 127.1, 126.93, 126.97, 126.1, 125.1, 121.6, 121.2, 111.6, 101.2, 99.7 ppm; UV–visible (CH₂Cl₂) λ_{max} (log ε): 420 (5.08), 517 (3.91), 552 (3.91), 598 (3.16), 654 (4.34) nm; HR-MS (ESI+, 100% CH₃CN, TOF): *m/z* calcd for C₄₇H₃₈N₅O₂ (MH⁺): 704.3026, found 704.3009.

meso-Tetraphenyl-3-N-dibenzylamine-2-oxachlorin (13-N(Bn)₂). Prepared according to the general procedure from 11H₂ (10.7 mg, 0.017 mmol) and dibenzylamine (1 mL) in 70% isolated yield (9.6 mg): *R_f* (silica–CH₂Cl₂) = 0.96; ¹H NMR (300 MHz, CDCl₃, δ): 8.54–8.56 (m, 1H), 8.39–8.44 (m, 2H), 8.34–8.35 (m, 1H), 8.26–8.28 (m, 1H), 7.98–8.15 (m, 7H), 7.84–7.89 (m, 1H), 7.71–7.71 (m, 12H), 7.49–7.55 (m, 1H), 7.28 (s, 1H), 7.11–7.12 (br, 5H), 6.84–6.86 (m, 4H), 3.47–3.61 (m, 4H), –0.33 (s, 1H), –0.70 (s, 1H) ppm; UV–visible (CH₂Cl₂) λ_{max} (log ε): 420 (5.16), 518 (3.97), 555 (3.97), 600 (3.69), 655 (4.39) nm; HR-MS (ESI+, 100% CH₃CN, TOF): *m/z* calcd for C₅₇H₄₄N₅O (MH⁺): 814.3546, found 814.3590.

■ ASSOCIATED CONTENT

Supporting Information

¹H, ¹³C NMR, and IR spectra of all compounds and experimental details to the crystal structure determination of 5H₂, 5aZn, 12H₂, 13-OMe, and 15–II-Zn, including the cif files. This material is available free of charge via the Internet at <http://pubs.acs.org>.

■ AUTHOR INFORMATION

Corresponding Author

*Fax: (+1) 860 486-2981. Tel: (+1) 860 486-2743. E-mail: c.bruckner@uconn.edu.

Present Address

‡Center for Systems Biology, Massachusetts General Hospital, Boston, MA 02114, United States.

Notes

The authors declare no competing financial interest.

■ ACKNOWLEDGMENTS

This work was supported by the US National Science Foundation (CHE-0517782 and CHE-1058846 to CB). The 400 MHz NMR used was supported by the NSF (CHE-1048717). The diffractometer at YSU was funded by NSF grant 0087210, by Ohio Board of Regents grant CAP-491, and by YSU. The theoretical studies were supported by grants from the National Institutes of Health (GM-34548) and the National Science Foundation (EMT-08517; both to R.R.B.). C.J.Z. acknowledges the National Science Foundation (CHE-0840446) for funds used to purchase the diffractometer at Akron used in this work. We thank Renee Rubenstein, Eileen Meehan, Alison Rossi (supported by a UConn SURF grant), Douglas Mooney (supported by NSF-REU grant CHE-0754580), John Haskoor (supported by a UConn SURF grant), and Kim Panther (supported by NSF-REU grant CHE-1062946) for experimental assistance.

■ REFERENCES

- (1) For a representative synthetic light-harvesting systems, see, e.g.: For Tomizaki, K.; Loewe, R. S.; Kirmaier, C.; Schwartz, J. K.; Retsek, J. L.; Bocian, D. F.; Holten, D.; Lindsey, J. S. *J. Org. Chem.* **2002**, *67*, 6519–6534 and references therein.
- (2) Lindsey, J. S. In *Porphyrim Handbook*; Kadish, K. M., Smith, K. M., Guillard, R., Eds.; Academic Press: San Diego, 2000; Vol. 1, pp 45–118.
- (3) Crossley, M. J.; King, L. G. *J. Chem. Soc., Chem. Commun.* **1984**, 920–922.
- (4) Gouterman, M.; Hall, R. J.; Khalil, G. E.; Martin, P. C.; Shankland, E. G.; Cerny, R. L. *J. Am. Chem. Soc.* **1989**, *111*, 3702–3707.
- (5) Khalil, G.; Gouterman, M.; Ching, S.; Costin, C.; Coyle, L.; Gouin, S.; Green, E.; Sadilek, M.; Wan, R.; Yearyea, J.; Zelelow, B. J. *Porphyrim Phthalocyanines* **2002**, *6*, 135–145.
- (6) Jayaraj, K.; Gold, A.; Austin, R. N.; Ball, L. M.; Terner, J.; Mandon, D.; Weiss, R.; Fischer, J.; DeCian, A.; Bill, E.; Müther, M.; Schünemann, V.; Trautwein, A. X. *Inorg. Chem.* **1997**, *36*, 4555–4566.
- (7) Köpke, T.; Pink, M.; Zaleski, J. M. *Chem. Commun.* **2006**, 4940–4942.
- (8) McCarthy, J. R.; Melfi, P. J.; Capetta, S. H.; Brückner, C. *Tetrahedron* **2003**, *59*, 9137–9146.
- (9) Akhigbe, J.; Ryppa, C.; Zeller, M.; Brückner, C. *J. Org. Chem.* **2009**, *74*, 4927–4933.
- (10) Cetin, A.; Ziegler, C. J. *Dalton Trans.* **2005**, 25–26.
- (11) Rahimi, R.; Tehrani, A. A.; Fard, M. A.; Sadegh, B. M. M.; Khavasi, H. R. *Catal. Commun.* **2009**, *11*, 232–235.
- (12) (a) Zelelow, B.; Khalil, G. E.; Phelan, G.; Carlson, B.; Gouterman, M.; Callis, J. B.; Dalton, L. R. *Sens. Actuators, B* **2003**, *96*, 304–314. (b) Gouterman, M.; Callis, J.; Dalton, L.; Khalil, G.; Mebarki, Y.; Cooper, K. R.; Grenier, M. *Meas. Sci. Technol.* **2004**, *15*, 1986–1994. (c) Khalil, G. E.; Costin, C.; Crafton, J.; Jones, G.; Grenoble, S.; Gouterman, M.; Callis, J. B.; Dalton, L. R. *Sens. Actuators, B* **2004**, *97*, 13–21.
- (13) (a) Gouterman, M. *J. Chem. Educ.* **1997**, *74*, 697–702. (b) Schäferling, M. *Angew. Chem., Int. Ed.* **2012**, *51*, 3532–3554.
- (14) Khalil, G. E.; Daddario, P.; Lau, K. S. F.; Imtiaz, S.; King, M.; Gouterman, M.; Sidelev, A.; Puran, N.; Ghandehari, M.; Brückner, C. *Analyst* **2010**, *135*, 2125–2131.
- (15) McCarthy, J. R.; Jenkins, H. A.; Brückner, C. *Org. Lett.* **2003**, *5*, 19–22.
- (16) Brückner, C.; Rettig, S. J.; Dolphin, D. *J. Org. Chem.* **1998**, *63*, 2094–2098.
- (17) Lara, K. K.; Rinaldo, C. K.; Brückner, C. *Tetrahedron* **2005**, *61*, 2529–2539.
- (18) Banerjee, S.; Zeller, M.; Brückner, C. *J. Org. Chem.* **2010**, *75*, 1179–1187.

- (19) Samankumara, L. P.; Zeller, M.; Krause, J. A.; Brückner, C. *Org. Biomol. Chem.* **2010**, *8*, 1951–1965.
- (20) The numbering of chlorins as 2,3-dihydroporphyrins is against IUPAC recommendations (a chlorin is a 7,8-dihydroporphyrin; IUPAC-IUB Joint Commission on Biochemical Nomenclature, *Pure Appl. Chem.* **1987**, *59*, 779–832.) but frequently used, intuitive, and convenient.
- (21) (a) Starnes, S. D.; Rudkevich, D. M.; Rebeck, J., Jr. *J. Am. Chem. Soc.* **2001**, *123*, 4659–4669. (b) Sutton, J. M.; Clarke, O. J.; Fernandez, N.; Boyle, R. W. *Bioconjugate Chem.* **2002**, *13*, 249–263. (c) Rancan, F.; Wiehe, A.; Noebel, M.; Senge, M. O.; Omari, S. A.; Boehm, F.; John, M.; Roeder, B. J. *Photochem. Photobiol.* **2005**, *78*, 17–28. (d) Choi, Y.; McCarthy, J. R.; Weissleder, R.; Tung, C. H. *ChemMedChem* **2006**, *1*, 458–463. (e) Al-Omari, S. *Biomed. Mater.* **2007**, *2*, 107–115.
- (22) MacAlpine, J. K.; Boch, R.; Dolphin, D. J. *Porphyryns Phthalocyanines* **2002**, *6*, 146–155.
- (23) Wang, T. Y.; Chen, J. R.; Ma, J. S. *Dyes Pigm.* **2002**, *52*, 199–208.
- (24) (a) Akhigbe, J.; Haskoor, J.; Zeller, M.; Brückner, C. *Chem. Commun.* **2011**, *47*, 8599–8601. (b) Akhigbe, J.; Peters, G.; Zeller, M.; Brückner, C. *Org. Biomol. Chem.* **2011**, *9*, 2306–2313. (c) Brückner, C.; Götz, D. C. G.; Fox, S. P.; Rypa, C.; McCarthy, J. R.; Bruhn, T.; Akhigbe, J.; Banerjee, S.; Daddario, P.; Daniell, H. W.; Zeller, M.; Boyle, R. W.; Bringmann, G. *J. Am. Chem. Soc.* **2011**, *133*, 8740–8752.
- (25) Ogikubo, J.; Brückner, C. *Org. Lett.* **2011**, *13*, 2380–2383.
- (26) The range from ~650 to 1300 nm in which tissue has the largest depth of penetration; the wavelength of maximum penetration of breast tissue is ~725 nm: Cerussi, A. E.; Berger, A. J.; Bevilacqua, F.; Shah, N.; Jakubowski, D.; Butler, J.; Holcombe, R. F.; Tromberg, B. J. *Acad. Radiol.* **2001**, *8*, 211–218.
- (27) (a) Sternberg, E. D.; Dolphin, D.; Brückner, C. *Tetrahedron* **1998**, *54*, 4151–4202. (b) Bonnett, R. *Chemical Aspects of Photo-dynamic Therapy*; Gordon & Breach: Langhorne, PA, 2000. (c) Pandey, R. K.; Zheng, G. In *The Porphyrin Handbook*; Kadish, K. M., Smith, K. M., Guillard, R., Eds.; Academic Press: San Diego, 2000; Vol. 6, pp 157–230.
- (28) *Chlorophylls and Bacteriochlorophylls*; Grimm, B., Porra, R. J., Rüdinger, W., Scheer, H., Eds.; Springer: Dordrecht, NL, 2006; Vol. 25.
- (29) (a) Flitsch, W. *Adv. Heterocycl. Chem.* **1988**, *43*, 73–126. (b) Montforts, F.-P.; Gerlach, B.; Hoepfer, F. *Chem. Rev.* **1994**, *94*, 327–347. (c) Shanmugathasan, S.; Edwards, C.; Boyle, R. W. *Tetrahedron* **2000**, *56*, 1025–1046. (d) Galezowski, M.; Gryko, D. *Curr. Org. Chem.* **2007**, *11*, 1310–1338. (e) Taniguchi, M.; Mass, O.; Boyle, P. D.; Tang, Q.; Diers, J. R.; Bocian, D. F.; Holten, D.; Lindsey, J. S. *J. Mol. Struct.* **2011**, *979*, 27–45. (f) Taniguchi, M.; Kim, H.-J.; Ra, D.; Schwartz, J. K.; Kirmaier, C.; Hindin, E.; Diers, J. R.; Prathapan, S.; Bocian, D. F.; Holten, D.; Lindsey, J. S. *J. Org. Chem.* **2002**, *67*, 7329–7342. (g) Taniguchi, M.; Ptaszek, M.; McDowell, B. E.; Boyle, P. D.; Lindsey, J. S. *Tetrahedron* **2007**, *63*, 3850–3863. (h) Taniguchi, M.; Ptaszek, M.; McDowell, B. E.; Lindsey, J. S. *Tetrahedron* **2007**, *63*, 3840–3849. (i) Kee, H. L.; Kirmaier, C.; Tang, Q.; Diers, J. R.; Muthiah, C.; Taniguchi, M.; Laha, J. K.; Ptaszek, M.; Lindsey, J. S.; Bocian, D. F.; Holten, D. *Photochem. Photobiol.* **2007**, *83*, 1125–1143. (j) Kee, H. L.; Kirmaier, C.; Tang, Q.; Diers, J. R.; Muthiah, C.; Taniguchi, M.; Laha, J. K.; Ptaszek, M.; Lindsey, J. S.; Bocian, D. F.; Holten, D. *Photochem. Photobiol.* **2007**, *83*, 1110–1124. (k) Laha, J. K.; Muthiah, C.; Taniguchi, M.; McDowell, B. E.; Ptaszek, M.; Lindsey, J. S. *J. Org. Chem.* **2006**, *71*, 4092–4102. (l) Ruzie, C.; Krayer, M.; Lindsey, J. S. *Org. Lett.* **2009**, *11*, 1761–1764.
- (30) Brückner, C.; McCarthy, J. R.; Daniell, H. W.; Pendon, Z. D.; Ilagan, R. P.; Francis, T. M.; Ren, L.; Birge, R. R.; Frank, H. A. *Chem. Phys.* **2003**, *294*, 285–303.
- (31) McCarthy, J. R.; Perez, M. J.; Brückner, C.; Weissleder, R. *Nano Lett.* **2005**, *5*, 2552–2556.
- (32) Zeller, M.; Hunter, A. D.; McCarthy, J. R.; Capetta, S. H.; Brückner, C. *J. Chem. Crystallogr.* **2005**, *35*, 935–942.
- (33) Tércio, J.; Ferreira, B.; Cruz, W. O.; Vieira, P. C.; Yonashiro, M. *J. Org. Chem.* **1987**, *52*, 3698–3699.
- (34) Vogel, A. I.; Tatchell, A. R.; Furnis, B. S.; Hannaford, A. J.; Smith, P. W. G. *Vogel's Textbook of Practical Organic Chemistry*, 5th ed.; Pearson: Edinburgh Gate, 1989.
- (35) National Institute for Occupational Health and Safety Registry of Toxic Effects of Chemical Substances (RTECS): RN1140000; TSCA 8(b) inventory.
- (36) Hyland, M. A.; Morton, M. D.; Brückner, C. *J. Org. Chem.* **2012**, *77*, 3038–3048.
- (37) CSD code TPHPOR04
- (38) Jentzen, W.; Song, X.-Z.; Shelnutz, J. A. *J. Phys. Chem. B.* **1997**, *101*, 1684–1699.
- (39) Senge, M. O. In *Porphyry Handbook*; Kadish, K. M., Smith, K. M., Guillard, R., Eds.; Academic Press: San Diego, 2000; Vol. 10, p 1–218.
- (40) CSD code PYZNPO10.
- (41) (a) Inoue, S.; Takeda, N. *Bull. Chem. Soc. Jpn.* **1977**, *50*, 984–986. (b) Buchler, J. W. In *Porphyryns and Metalloporphyryns*, 2nd ed.; Smith, K. M., Ed.; Elsevier Scientific Publishing Company: Amsterdam, 1975; pp 157–232.
- (42) Gouterman, M. In *The Porphyryns*; Dolphin, D., Ed.; Academic Press: New York, 1978; Vol. 3, pp 1–165.
- (43) See, for example, the studies relating to the optical properties of the chlorins synthesized by Lindsey and co-workers, ref 29e through 29 L, and references therein
- (44) Pawlicki, M.; Latos-Grazynski, L. *Chem.–Eur. J.* **2003**, *9*, 4650–4660.
- (45) Pawlicki, M.; Latos-Grazynski, L. *J. Org. Chem.* **2005**, *70*, 9123–9130.
- (46) (a) Grzegorzec, N.; Pawlicki, M.; Latos-Grazynski, L. *J. Org. Chem.* **2009**, *74*, 8547–8553. (b) Grzegorzec, N.; Pawlicki, M.; Szterenber, L.; Latos-Grazynski, L. *J. Am. Chem. Soc.* **2009**, *131*, 7224–7225.
- (47) (a) Martin, C. H.; Birge, R. R. *J. Phys. Chem. A* **1998**, *102*, 852–860. (b) Ren, L.; Martin, C. H.; Wise, K. J.; Gillespie, N. B.; Luecke, H.; Lanyi, J. K.; Spudich, J. L.; Birge, R. R. *Biochemistry* **2001**, *40*, 13906–13914. (c) Shima, S.; Ilagan, R. P.; Gillespie, N.; Sommer, B. J.; Hiller, R. G.; Sharples, F. P.; Frank, H. A.; Birge, R. R. *J. Phys. Chem. A* **2003**, *107*, 8052–8066.
- (48) (a) Miyahara, T.; Nakatsuji, H.; Hasegawa, J.; Osuka, A.; Aratani, N.; Tsuda, A. *J. Chem. Phys.* **2002**, *117*, 11196–11206. (b) Nakatsuji, H.; Hirao, K. *J. Chem. Phys.* **1978**, *68*, 2053–2065. (c) Nakatsuji, H. *Chem. Phys. Lett.* **1991**, *177*, 331–337.
- (49) Dunning, T. H., Jr.; Hay, P. J. In *Modern Theoretical Chemistry*; Schaefer, H. F., Ed.; Plenum, New York, 1976; Vol. 3, pp 1–28.
- (50) Premvardhan, L.; Sandberg, D. J.; Fey, H.; Birge, R. R.; Buchel, C.; Grondelle, R. v. *J. Phys. Chem. B* **2008**, *112*, 11838–11853.
- (51) Adler, A. D.; Longo, F. R.; Finarelli, J. D.; Goldmacher, J.; Assour, J.; Korsakoff, L. *J. Org. Chem.* **1967**, *32*, 476.
- (52) (a) Adler, A. D.; Longo, F. R.; Kampas, F.; Kim, J. J. *Inorg. Nucl. Chem.* **1970**, *32*, 2443–2445. (b) Dean, M. L.; Schmink, J. R.; Leadbeater, N. E.; Brückner, C. *Dalton Trans.* **2008**, 1341–1345.
- (53) Crossley, M. J.; Hambley, T. W.; King, L. G. *Bull. Soc. Chim. Fr.* **1996**, *133*, 735–742.